Design and Development of Biodegradable Zwitterionic Polymers for Drug Delivery in Cancer

A Thesis

submitted to

Indian Institute of Science Education and Research Pune in partial fulfilment of the requirements for the Masters Degree Programme

by

SANCHI

Indian Institute of Science Education and Research Pune

Dr. Homi Bhabha Road,

Pashan, Pune 411008, INDIA.

11 April 2024

Supervisor: Prof. M. Jayakannan

Certificate

This is to certify that this dissertation entitled **"Design and Development of Biodegradable Zwitterionic Polymers for Drug Delivery in Cancer"** towards the partial fulfilment of the MSc degree programme at the Indian Institute of Science Education and Research, Pune represents study/work carried out by **Sanchi** at Indian Institute of Science Education and Research under the supervision of **Professor M. Jayakannan**, Department of Chemistry, during the academic year 2023-2024.

Name of your Guide: Prof.
M. Jayakannan

Committee:

Name of your Guide: Prof. M. Jayakannan

Name of Your TAC: Prof. S.G. Srivatsan

Signature of the supervisor 

`

This thesis is dedicated to my mother

Declaration

I hereby declare that the matter embodied in the report entitled **''Design and Development of Biodegradable Zwitterionic Polymers for Drug Delivery in Cancer"** are the results of the work carried out by me at the Department of Chemistry, Indian Institute of Science Education and Research, Pune, under the supervision of **Prof M. Jayakannan** and the same has not been submitted elsewhere for any other degree.

Your Name: Sanchi

Date: 11-04-24

Signature of the student 

Table of Contents

Abstract…….....7

Acknowledgments ……..8

Chapter 1 Introduction……..9

Chapter 2 Materials and Methods……14

2.1 Materials
2.2 Methods
2.3 Synthesis
2.4 Self-assembly of Polymers
2.5 pH dependent studies of Polymers
2.6 Dye Encapsulation in the Zwitterionic Polymers

Chapter 3 Results and Discussion……..26
3.1 Synthesis and Characterization of γ-substituted Monomers
3.2 Synthesis and Characterization of 1-undecyl-1H-imidazole
3.3 Synthesis and Characterization of Linear Polymers
3.4 Synthesis and Characterization of Star Polymers
3.5 Molecular weight estimation and Thermal stability of Polymers
3.6 Self-assemblies of charged polymer nanoparticles
3.7 pH dependent studies of charged polymers
3.8 Dye encapsulation in the zwitterionic nano-scaffolds

Chapter 4 Conclusion……44

References……45

List of Figures

Figure	Title	Page No.
Fig 1.1	Polymer nanoparticles for targeted drug delivery	9
Fig 1.2	Zwitterionic polymers in biological systems	10
Fig 1.3	Zwitterionic Building Blocks	11
Fig 1.4	Biodegradable polymers	12
Fig.1.5	Different initiators based on arm numbers	12
Fig 3.1	Monomer Synthesis Scheme	26
Fig 3.2	^{1}H NMR of Compound 1, 2 and Monomer M1	27
Fig 3.3	^{1}H NMR of Compound 3	27
Fig 3.4	^{1}H NMR of Compound 4 and Monomer M2	28
Fig 3.5	^{1}H NMR of Compound I-11	28
Fig 3.6	Reaction Scheme of Linear Polymers	29
Fig 3.7	^{1}H NMR of Linear Homopolymer P1	30
Fig 3.8	^{1}H NMR of Linear Block copolymer P2	30
Fig 3.9	^{1}H NMR of Linear Cationic Polymer CP1	30
Fig 3.10	^{1}H NMR of Linear Anionic Polymer AP1	31
Fig 3.11	^{1}H NMR of Linear Zwitterionic Polymer ZP1	31
Fig 3.12	Reaction Scheme of Star Polymer	32
Fig 3.13	^{1}H NMR of Star Homopolymer P3	33
Fig 3.14	^{1}H NMR of Star Block copolymer P4	33
Fig 3.15	^{1}H NMR of Star Cationic Polymer CP2	34
Fig 3.16	^{1}H NMR of Star Anionic Polymer AP2	34
Fig 3.17	^{1}H NMR of Star Zwitterionic Polymer ZP2	35
Fig 3.18	SEC Plots	37
Fig 3.19	TGA Analysis	37
Fig 3.20	DSC plots	38
Fig 3.21	Self-assembly studies	38
Fig 3.22	Nanoparticle characterization using DLS	39
Fig 3.23	Nanoparticle characterization using Zeta Potential	40
Fig 3.24	pH dependent size studies	42
Fig 3.25	pH dependent charge studies	42
Fig 3.26	Dye encapsulation in zwitterionic scaffolds	43
Fig 3.27	HPTS loaded Zwitterionic nanoparticles	43

List of Table

Table	Title	Page No.
Table 1	Molecular weight and thermal properties	36
Table 2	Tabular data for dye encapsulation	43

Abstract:

Zwitterionic polymers are well known for their wide range of biomedical applications such as drug delivery, protein conjugation, nanoparticle formation, etc. This thesis is aimed at "Designing and Developing Enzymatically Biodegradable Zwitterionic Block Copolymers for Drug Delivery in Cancer." For this purpose, two γ-substituted caprolactone monomers were tailor-made by multi-step organic synthesis. Ring-opening polymerization (ROP) technique was employed to achieve linear, and star (6-arm) shaped block copolymer based several architectures. Further, linear and star polymers were post-modified to yield cationic, anionic and zwitterionic amphiphilic structures. The chain length in linear and each arm of star architecture is kept same to understand the role of topology. Monomers and polymers were characterized using ^{1}H NMR, ^{13}C NMR, FT-IR, mass spectra. The molecular weight of polymers was estimated using Gel Permeation Chromatography (GPC). Thermal properties were studied by thermogravimetric analysis (TGA) and differential scanning calorimetry (DSC). The polymers were found to be stable up to 250 °C and semicrystalline to amorphous in nature. Self-assembly in aqueous medium showed formation of aggregated nano assembles having hydrodynamic diameter in the range of 60-340 nm for linear polymers and 30-200 nm for star polymers. pH dependent size and zeta potential measurements revealed formation of stable nano-assemblies. HPTS (biomarker) dye was encapsulated in the linear and star zwitterionic with excellent dye loading capacities of 3%. HPTS loaded nanoparticles were characterized for size and zeta potential analysis.

Acknowledgments

I would like to acknowledge my supervisor Prof. M. Jayakannan for their constant support and guidance during my journey of MSc thesis. He always motivated me and gave me the opportunity to explore new research domains and express my ideas.

I would like to extend warm gratitude to my TAC member Prof. S.G Srivatsan, for their valuable time and excellent suggestions during evaluation of my mid-term report to improve the project direction.

I would like to special thanks to my project mentor Shahid Khan Pathan for helping me constantly and building fruitful conclusions throughout this project. Further, my lab members assisted me in learning new techniques and enlightened my knowledge for the successful completion of my thesis work. I thank all my lab seniors Dr. Mohammed Khuddus, Kambale Parshuram, Utreshwar Gavhane, Kajal Singh, Mishika Virmani for teaching me and developing new skills. I thank all my past lab seniors Dr. Ruma Ghosh, Dr. Mehak Malhotra, Dr. Bapurao Surnar, whose contribution to polymer chemistry guided me a lot in fabricating new ideas. I would like to acknowledge my labmates Ashutosh Shirodkar, Rhujal Mokal, Vaishak Bhat, Akshay Nagrikar, Pawar Bhushan and Sunidhi Singh for sharing valuable research experience that helped to develop new skills.

I am glad to extend special thanks to my family members father Pawan Kumar, mother Poonam and brother Piyush for holding me up during this journey. I am grateful for the friends who were always there to listen to my views patiently and motivate me to give my best.

Chapter 1 **Introduction**

Cancer is one of the life threatening diseases with highest mortality rate. The limitations of chemotherapy and side effects of the available drugs on human health have made it vital to develop and improve technology in this regard. The nanoparticles are employed as a vehicle for a stimuli-responsive drug delivery systems to obtain high efficiency.[1] Self-assembled polymers are an excellent nanocarrier for drug delivery applications due to their tunable properties and stimuli-responsive nature.[2] The excellent increase in drug circulation time and bioavailability are favored for polymer nanocarriers due to Enhanced permeability and retention (EPR) effect.[3]

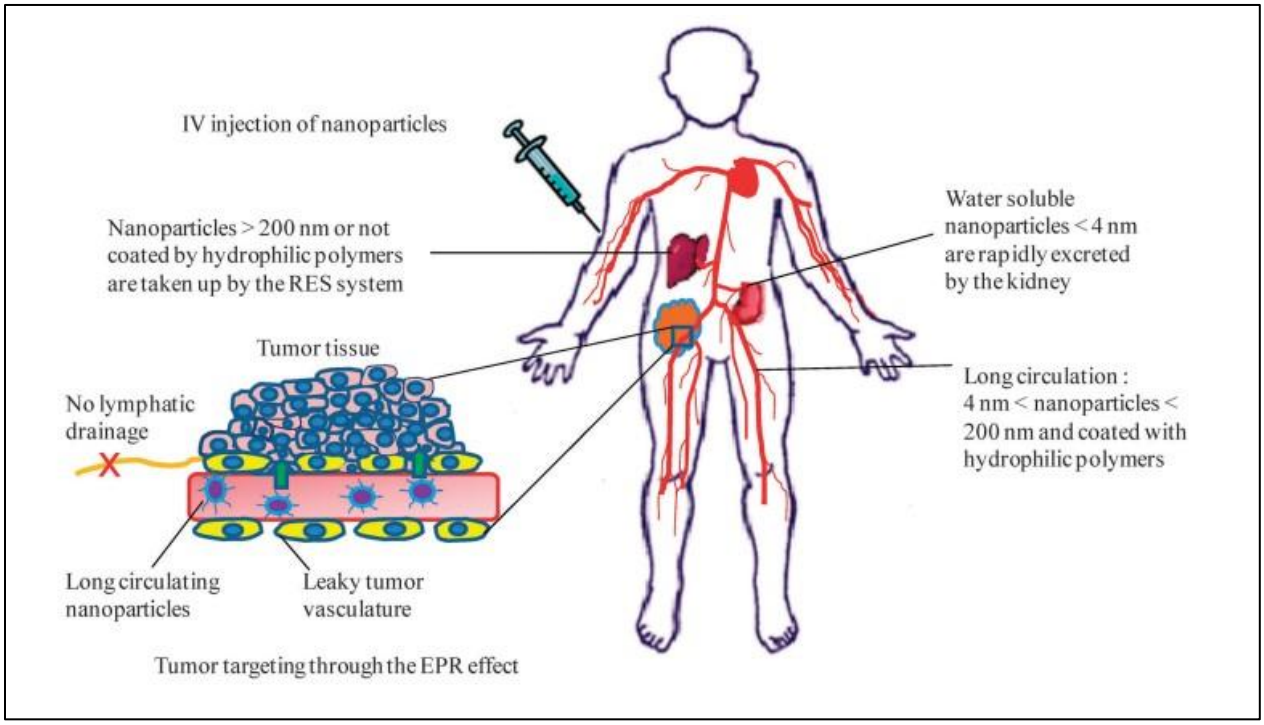

Fig 1.1 Polymer nanoparticles for targeted drug delivery
Adapted from Chem. Commun., ***2011***, *47, 9572–9587*

The idea of mimicking nature, motivated by natural biological systems such as lipid membrane models, model protein, and amino acids, Zwitterionic polymers evolve the designing and fabrication of new architectures. Zwitterionic polymers have become the great interest for researchers and many developments have been done in this regard.[4] This progress strengthens their application in biological systems such as nanoparticle conjugation, hydrogels, protein conjugation, etc.

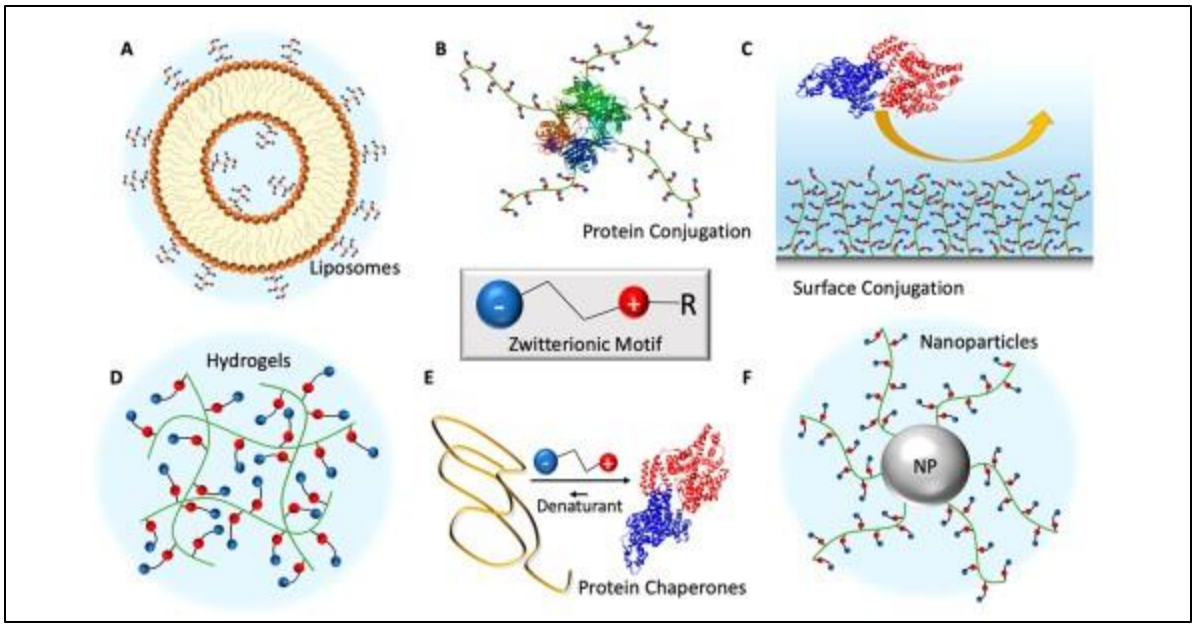

Fig 1.2 Zwitterionic polymers in biological systems

Adapted from Biomacromolecules ***2020*** 21 *(7), 2557-2573*

The presence of equal cationic and anionic groups in the zwitterionic polymers induces net electroneutrality. Zwitterionic polymer shows high polarity, high charge,[5] superhydrophilicity,[6] antifouling property,[7] better shielding power and high biocompatibility. Zwitterionic polymers interact with water molecules through ionic interactions and form stable and denser hydration layer. Thus, prevents non-specific interactions, bio adherence and provides protein stabilization.

The interaction between zwitterionic chains can be interpreted with the help of Hofmeister series, where the addition of salts disturbs the interaction and results in the enhancement of solubility. The addition of salt changes the collapsed confirmation of polymers to expanded form due to the variation in dipole moment and electrostatic interaction. At the isoelectric point, the balance between positive and negative charges occurs in the polymer backbone. Deviation from isoelectric point results in electrostatic repulsion and increase in the swelling rate. Zwitterionic nanoparticles designed with stimuli-responsive (pH responsive, temperature, light, enzyme specific) features show more circulation time, low cytotoxicity and increase in cellular uptake.[8] Due to the diverse properties of zwitterionic polymers, they have been widely exploited in range of biomedical applications in drug-delivery systems, enhancement in drug loading efficiency and reduce cytotoxicity and classified as smart or intelligent polymers. Amphiphilic triblock poly(ε-caprolactone)-poly(diethylaminoethyl methacrylate)-poly(sulfobetaine methacrylate) (PSBMA-PDEA-PCL) possessing pH responsive nature, was reported by Zhai et. al.[9] The fabrication of pH sensitive units in the polymer architecture offers the effective and controlled release of the drug in the cytoplasm.

Zwitterionic polymers are basically classified into two types: Polybetaines and Polyampholytes. Polybetaines are the macromolecules containing both positive and negative charge present together in the same repeating unit, while in case of Polyampholytes, each monomeric unit is present as an independent moiety carrying positively and negatively charged subunit in the polymer backbone. The well explored zwitterionic building blocks reported in the literature includes sulfobetaine (SB), carboxybetaine (CB), phosphorylcholine (PC).[10] Controlled Radical Polymerization is generally employed to achieve the zwitterionic polymers. The poly(peptides) and amino acids are another method for incorporation of zwitterionic polymers.[11]

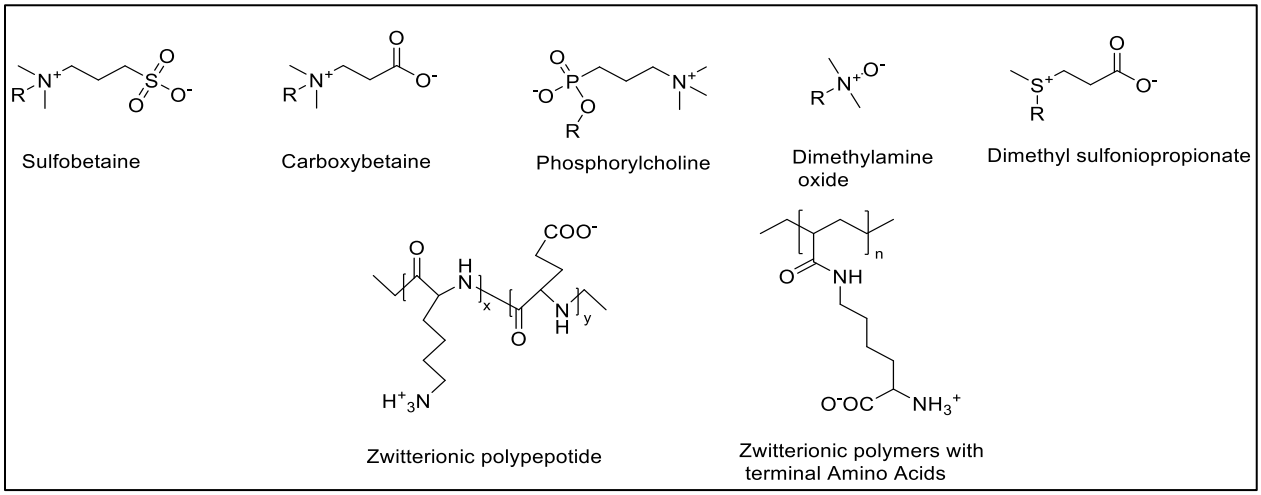

Fig 1.3. Zwitterionic Building Blocks

Mostly reports for zwitterionic polymers are based on acrylate chemistry. Synthetic polymers are toxic as well as non-biodegradable in nature. Therefore, the novel idea of developing zwitterionic biodegradable polymers as nanocarriers has become a concern for researchers. Polycarbonates, Polycaprolactones, Polyvalerolactones, Polylactides, Polyureas and Polyaminoacids are generally explored biodegradable polymers in this regard. Emma et. al. installed zwitterionic moiety by using thio-ene chemistry for the stabilization of insulin by implementing the allyl functionalized Caprolactone, Carbonate, Lactide and Valerolactone polymers.[12]

Polyesters are an important class of polymers for the development of environmentally friendly polymers, generally degraded by ester hydrolysis and show enzymatic degradation.[13] The idea of developing polyesters based zwitterionic polymers is one of the curious topics to be addressed. The strategies used to develop polyesters with modifications includes the designing of substituted monomers and another one includes the grafting of functional groups on the polyester backbone. Ring-Opening Polymerization (ROP) and melt polycondensation (MP) are employed to fabricate the functionalized bio-based polyesters.[14] Further, the Click Copper Catalyzed Azide-Alkyne Huisgen's Cycloaddition has also been carried out and proven to be an efficient method to get functionalized polyesters.[15] Cao et. al reported biodegradable PCL based sulfobetaine polymers with excellent biocompatibility and biodegradability.[16] In this report, amphiphilic PCL-APS-PCL triblock copolymers, consisting of N,N'-bis (2-hydroxyethyl) methylamine

ammonium propane sulfonate (APS) as hydrophilic unit and polycaprolactone as hydrophobic unit has proven to be novel candidate for anticancer treatment.

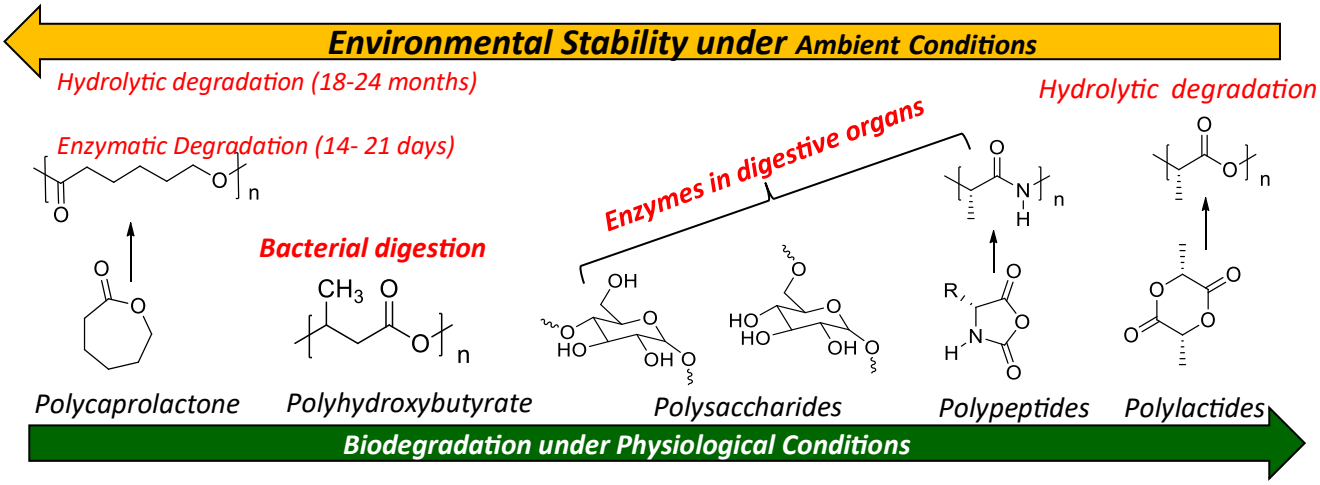

Fig 1.4 Biodegradable polymers

To develop amine based amphiphilic zwitterionic polymers, N-substituted aliphatic cyclic carbonates were fabricated by Venkataraman et. al. group for biomedical applications.[17]

The incorporation of zwitterionic moieties can be done by employing following polymerization techniques: Reversible-Deactivation Radical Polymerization (RDRP), step- growth polymerization, Ring-Opening Metathesis Polymerization (ROMP), post-polymerization and click chemistry.[18] Zwitterionic moieties having amphiphilic character are greatly influenced by the shape of polymer nano-micelles. The smartly engineering of star and linear shaped polymer substantially affect the micellar structure.[19] Topology of polymers tremendously alters the self-assembly and biomaterial properties. Various structures include dendrimers, comb, brush, star shaped, hyperbranched are well explored in the literature.[20] Poly(caprolactone) based systems are investigated depending on the multi arm architectures to fabricate well-defined macrostructures. The thermal and crystallinity of biodegradable polymers are greatly influenced by the arm number.[21] In contrast to linear polymers, the three-dimensional spherical structures of star polymers result in smaller hydrodynamic volume, less entanglement and drop in viscosity. Ren et. al reported star shaped Poly(ε-caprolactone)-b-Poly(L-lactide) copolymers by Ring Opening Polymerization to further study thermal and crystallinity properties.[22]

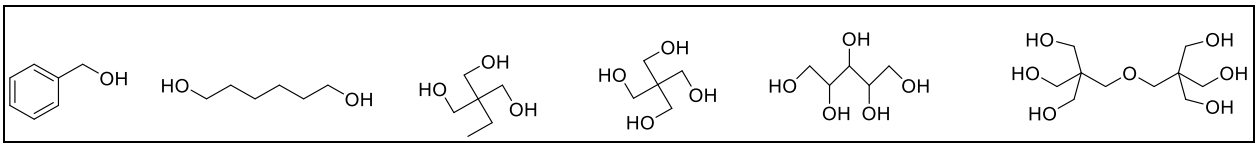

Fig 1.5 Different initiators based on arm number

Fabrication of refined polymer architectures with precise control on the structures has been a concern for modification of properties. Zwitterionic block copolymers with amphiphilic nature have shown promise for improved and modified features.[23] There is an excellent difference in the features of linear and star polymers such as stability, size, self-assembly and charges. The overall control in the polymer architecture influences its properties, drug loading content and its application in biomedical science.[24]

Bapurao et. al. reported pH sensitive carboxylic functionalized polycaprolactone block copolymer as drug delivery vehicle for controlled release of drugs.[25] Further, the approach has been taken forward by Mehak et. al. to investigate polymer topology of carboxyl substituted caprolactone and caprolactone based on random and block copolymers for anticancer treatment[26]. Ghosh et. al reported cationic amphiphilic enzymatic-biodegradable caprolactone for antimicrobial activity.[27,28] Mehak et. al also developed star-shaped unimolecular micelle based on caprolactone systems for application in blood brain barrier.[29]

The task of developing zwitterionic biodegradable polymers by combining the above two approaches has been taken in this report. The concept involved designing functionalized amphiphilic biobased linear and star charged polymers, mainly focusing on zwitterionic polymers.

Ring-Opening Polymerization has been explored for the substituted caprolactone monomers to engineer Linear and star (6-arm) polymer macrostructures. The number of units in linear polymer (M/I=10) have maintained to be constant in feed ratio with respect to each arm of star polymer (M/I=60), statistically 10 units on each arm. Further, post-modification has been done to yield zwitterionic polymers. The comparison between anionic, cationic and zwitterionic linear and star polymers has been made by studying pH dependent self-assemblies to get the deep knowledge about polymer topology. Additionally, linear and star zwitterionic polymers have been tested for drug loading capabilities by the encapsulation of anionic dye, HPTS and significant differences have been observed. Further, to constitute the proof of concept the development of zwitterionic polymers will be explored for cytotoxicity studies, degradation studies and in vivo models. This novel idea is based on the development of fully biodegradable based zwitterionic polymers that have very good potential for biomedical applications.

Chapter 2 Materials and Methods

2.1 Materials:

Chemicals were purchased from Sigma Aldrich : 1-Bromoundecane, 2-chloro ethanol, 1,4-Cyclohexanediol, dipantaerythritol, 8- hydroxypyrene-1,3,6-trisulfonic acid trisodium salt (HPTS), imidazole, m-chloroperbenzoic acid (m-CPBA), molecular sieves (4Å), potassium tert-butoxide, pyridinium chlorochromate (PCC), tert-butyl acrylate, tin(II) 2-ethylhexanoate ($Sn(oct)_2$), triethylene glycol monomethyl ether (TEG), Trifluoroacetic acid (TFA).
Locally purchased chemicals were: Na_2SO_4, $NaHCO_3$ $Na_2S_2O_3$, Na_2SO_4.
Solvents: Dichloromethane (DCM), Diethyl ether, Dimethylformamide (DMF), Dimethyl sulfoxide (DMSO), methanol, petroleum ether, Tetrahydrofuran (THF), Toluene.

2.2 Methods:

^1H, ^{13}C NMR spectra were measured in deuterated solvents $CDCl_3$ or DMSO-d_6 in 400 MHz Bruker spectrophotometer. The determination of molar masses of polymer were examined using Size Exclusion Chromatography (SEC) in $CHCl_3$ as eluent. Measurements were performed using polystyrene standards as calibration and Viscotek VE 1122 pump, Viscotek VE 3580 RI and 3210 UV-Vis detectors. TGA measurements were carried out at a rate of 10℃/min heating rate under a Nitrogen atmosphere using Perkin-Elmer thermal analyzer STA 6000 model. To determine thermal properties, Differential Scanning Calorimeter (DSC) were performed on TA Q2. Applied Bio systems 4800 PLUS MALDI TOF/TOF Analyzer was employed to record MALDI-TOF. HRMS-ESI-Q-time-of-flight LCMS (SynaptG2, Waters) was utilized to evaluate mass of small molecules. Malver Instrument, Zetasizer Nano ZS-90 apparatus operating using 633 nm red laser as light source at 90º angle was employed to analyze Dynamic Light Scattering (DLS) and Zeta Potential measurements.

2.3 Synthesis:

2.3.1 Synthesis of Monomers M1 and M2:

Synthesis of tert-butyl 3-((-4-hydroxycyclohexyl) oxy)propanoate (1): 1,4 Cyclohexane diol was dissolved (50 g, 430.44 mmoles) in Dry THF (500 mL). A catalytic amount of potassium t-butoxide was added to it (4 g, 12.28 mmoles). Kept it under reflux at 60℃ for 1 hour. Then, it was cooled to room temperature and t-butyl acrylate (44,13 g, 344.35 mmoles) in dry THF (100 mL) was added via dropping funnel. The reaction mixture was refluxed for 36 h at 70℃. THF was removed using rotary vapor and precipitation was done in DCM (200 mL) to remove unreacted diol. Viscous yellow liquid was obtained after the concentration of the filtered residue. The product was further purified by passing through silica column using ethyl acetate and hexane as eluent. Yield=26 g (31%).

^{1}H-NMR (400 MHz, $CDCl_3$) δ ppm: 3.65 (m, 3H, O−CH_2− and O−CH), 3.26−3.36 (m, 1H, CH−OH), 2.44 (t, 2H, −CH_2CO−), 1.97−1.82 (m, 4H, -CH2-), 1.63−1.30 (m, 4H, -CH_2-), 1.43 (s, 9H, -CH3). ^{13}C NMR (100 MHz, $CDCl_3$) δ ppm: 171.37, 80.60, 69.72, 68.60, 64.16, 63.74, 36.88, 32.72, 30.55, 29.34, 28.23, 27.65. FT-IR (cm^{-1}): 3618, 2961, 1715, 1413, 1361, 1252, 1157, 1106, 957, 895, 847, 756, 686, 603 and 516. HR-MS (ESI^+): m/z [M + Na+] for $C_{13}H_{24}O_4$ Calculated= 267.1572and Found =267.1512.

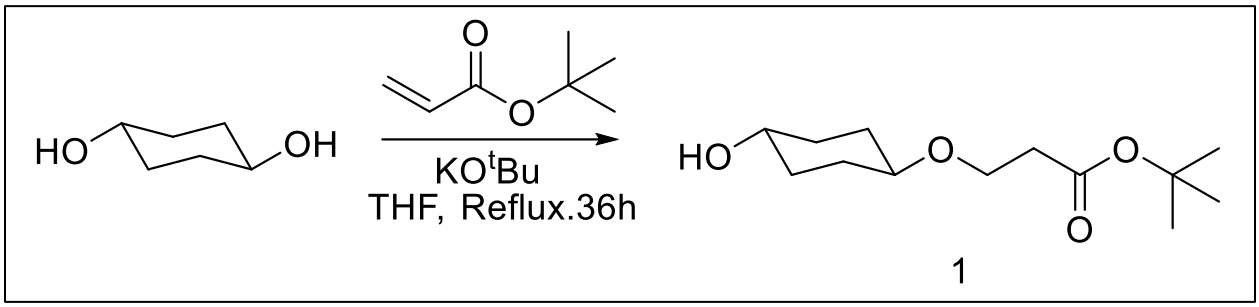

Scheme 2.1

Synthesis of t-Butyl-3-((4-oxocyclohexyl) oxy)-propanoate (2): The above Compound 1 (26 g, 106.41 mmoles) was dissolved in Dry DCM (500 mL). Molecular sieves($4A^0$) along with PCC (46 g, 212.8 mmoles) were added and kept on stirring at 25℃ overnight. Filtered the reaction mixture, washed with DCM and passed it through anhydrous Na_2SO_4. Further, purification was done using column chromatography in hexane and ethyl acetate system to obtain colorless liquid product. Yield=22.34 g (87%).

^{1}H-NMR (400 MHz, $CDCl_3$) δ ppm: 3.71 (m, 3H, O−CH_2- and O−CH-), 2.56 (m, 2H, −(CO)CH_2−), 2.48 (t, 2H, −CH_2−), 2.23 (m, 2H, −CH_2−), 2.06 (m, 2H, −CH_2−), 1.87 (m, 2H, −CH_2−), 1.42 (s, 9H, −CH_3). ^{13}C NMR (100 MHz, $CDCl_3$) δ ppm: 211.57, 171.14, 80.71, 73.08, 64.18, 37.15,36.71, 30.73, 28.19. FT-IR (cm^{-1}): 3618, 2961, 1718, 1413, 1361, 1252, 1157, 1106, 957, 895, 847, 756, 686, 603 and 516. HRMS (ESI+): m/z [M + Ma+] for $C_{13}H_{22}O_4$ Calculated= 265.1415 and Found =265.1415.

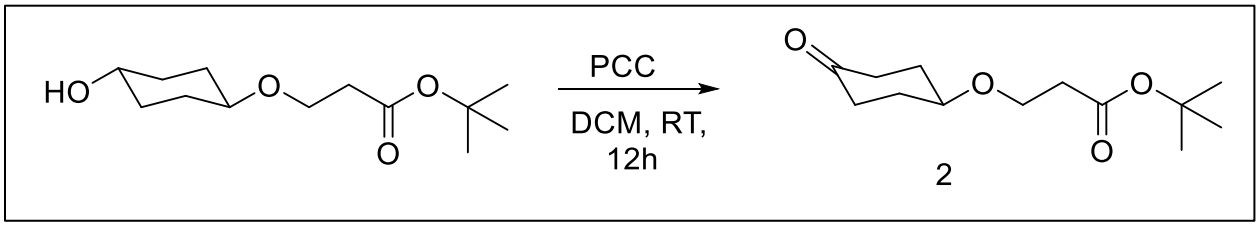

Scheme 2.2

Synthesis of tert-butyl 3-((7-oxooxepan-4-yl)oxy)propanoate (Monomer M1): Compound 2 (6 g, 24.7 mmoles) was dissolved in 150 mL DCM. To that, addition of $NaHCO_3$ (6 g, 74 mmoles) followed by mCPBA (8.5 g, 49.5 mmoles) was done. The reaction mixture was then kept for 24 h at 25℃. $NaHCO_3$ and $Na_2S_2O_3$ were employed to quench the reaction mixture and finally product was isolated in the organic layer. Dried

the organic layer on rotavapour and performed column chromatography to get pure product. Yield=5.6 g (89%).

^{1}H NMR (400MHz, $CDCl_3$) δ ppm: 4.49 (m, 1H, -CH-), 4.04 (m, 1H, -CH-), 3.66 (m, 3H,-CH-O), 2.90 (m, 1H, -CH-), 2.46 (t, 2H, CO-CH_2), 2.38 (m, 1H, -CH-), 1.99−1.76 (m, 4H, -CH-). ^{13}C NMR (100 MHz, $CDCl_3$) δ ppm: 176.14, 170.90, 80.71, 73.94, 63.95, 63.31, 36.48, 33.87, 28.11, 27.78, 27.32. FT-IR (cm^{-1}): 2925, 1725, 1456, 1393, 1366, 1253, 1155, 1100, and 1058. HRMS (ESI^+): m/z [M + Na+] for $C_{13}H_{32}O_5$ Calculated:281.1364 and Found: 281.1364.

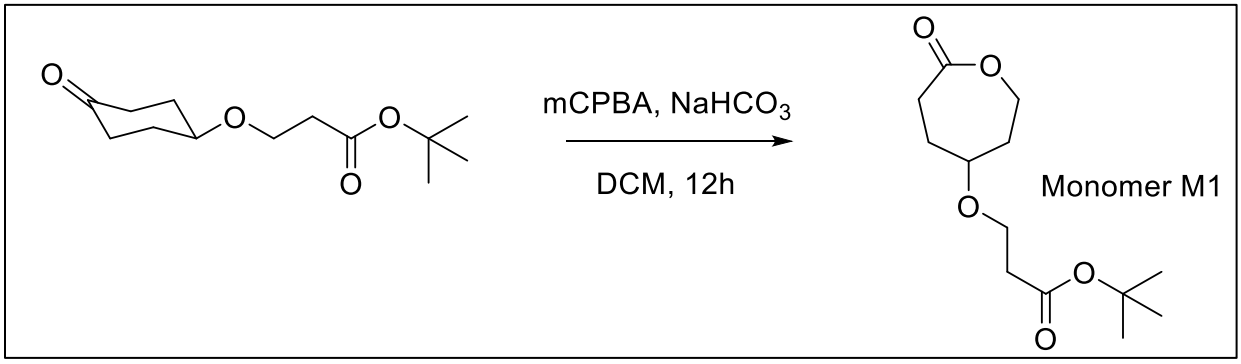

Scheme 2.3

Synthesis of 3-((4-oxocyclohexyl) oxy) propanoic acid (3): Compound 2 (22 g, 92.19 mmoles) was dissolved in Dry DCM (80 mL). To that, Trifluoroacetic acid was added dropwise at 0℃. Then, reaction mixture was kept on stirring at 25℃ for 2 h. To remove TFA, the reaction mixture was washed thrice with DCM. Finally, the crude product was purified by column chromatography in ethyl acetate and hexane to obtain a light-yellow liquid product. Yield=15 g (88%).

^{1}H NMR (400 MHz, CDCl3) δ ppm: 8.79 (s, 1H, -COOH), 3.77 (t, 2H, -O-CH_2-), 3.76 (m, 1H, -O-CH-), 2.65 (s, 2H, -CH_2-), 2.55 (m, 2H, −CH_2−), 2.25 (m, 2H, -CH_2−), 2.08 (m, 2H, −CH_2−), 1.90 (m, 2H, -O-CH_2−). ^{13}C NMR (100 MHz, $CDCl_3$) δ ppm: 211.89, 177, 72.78, 63.41, 36.99, 35.15, 30.51. FT-IR (cm-1): 3445, 2949, 1703, 1418, 1348, 1247, 1186, 1104, 1065, 956, 836, 735 and 587. HRMS (ESI^+): m/z [M + Na+] for $C_9H_{14}O_4$ Calculated: 209.0790 and Found: 209.0784.

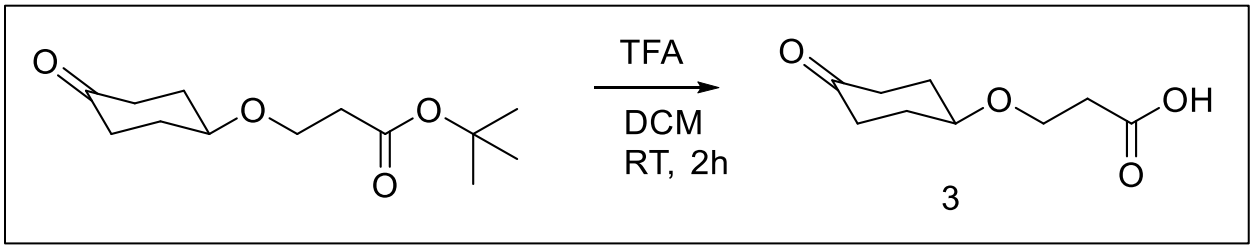

Scheme 2.4

Synthesis of 2-chloroethyl 3-((4-oxocyclohexyl) oxy) propanoate (4): Compound 3(15g, 80.55mmoles) and 2-chloroethanol (39 g,483.32 mmoles) were refluxed at 60℃ overnight. Extraction was done using ethyl acetate (150 mL) and distilled water (150 mL) to remove unreacted chloroethanol. The aqueous layer was washed again with ethyl acetate twice. The product was isolated in the organic layer and further colorless liquid product was obtained after purification by silica chromatography. Yield=12 g (60%).

^{1}H-NMR (400 MHz, CDCl3) δ ppm: 4.34 (t, 2H, O-CH_2), 3.79 (t, 2H, O-CH_2), 3.73 (m, 1H, -CH-), 3.68 (t, 2H, Cl-CH_2), 2.66 (t, 2H, $COCH_2$), 2.25 (m, 2H, -CH_2-), 2.08 (m, 2H, -CH_2-), 1.90 (m, 2H, -OCH_2-). ^{13}C NMR (100 MHz, $CDCl_3$) δ ppm: 211.32, 171.34, 73.03, 64.14, 63.60, 41.60, 37.25, 35.23, 30.41. FT-IR (cm-1): 3820, 3499, 2949, 2877, 1716, 1430, 1350, 1250, 1173, 1105, 1074, 1024, 960, 895, 821, 752, 666, 600, and 516. HRMS (ESI^+): m/z [M + Na+] for $C_{11}H_{17}ClO_4$ Calculated: 271.0713 and Found:271.0717.

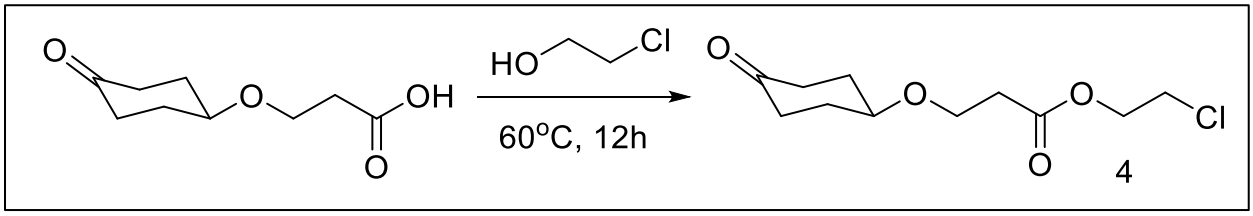

Scheme 2.5

Synthesis of 2-chloroethyl 3-((7-oxooxepan-4-yl) oxy) propanoate (Monomer M2): Compound 4 (7 g, 28.1mmoles) was dissolved in DCM (250 mL). To that, $NaHCO_3$(6g, 70.36mmoles) and m-CPBA (14.5g, 172.5mmoles) were added. Reaction mixture was kept on stirring at room temperature for 24 h. To quench the reaction mixture, saturated solution of $NaHCO_3$ was utilized, and the crude product was isolated in DCM. Passed the organic layer through anhydrous. Na_2SO_4 and DCM were removed using rotavapor. Finally, the column chromatography was done to obtain a product as pale-yellow liquid. Yield=4.5 g (60%).

^{1}H NMR (400 MHz, $CDCl_3$) δ ppm: 4.41 (m, 1H, -CH-), 4.30 (t, 2H, O-CH_2), 4.00 (m, 1H, -CH-), 3.66 (m, 5H,-CH-), 2.90 (m, 1H, -CH-), 2.58 (t, 2H, CO-CH_2), 2.38 (m, 1H, -CH-), 1.99−1.76 (m, 4H, -CH-). ^{13}C NMR (100 MHz, $CDCl_3$) δ ppm: 176.15, 171.31, 74.25, 64.26, 63.56, 63.37, 41.73, 35.21, 33.92, 27.85, 27.32. FT-IR (cm-1): 3057, 2881, 1731, 1433, 1355, 1265, 1182, 1120, 1069, 962, 896, 729, and 562. HRMS (ESI^+): m/z [M + H+] for $C_{11}H_{17}ClO_5$ Calculated: 265.0835 and Found:65.0838.

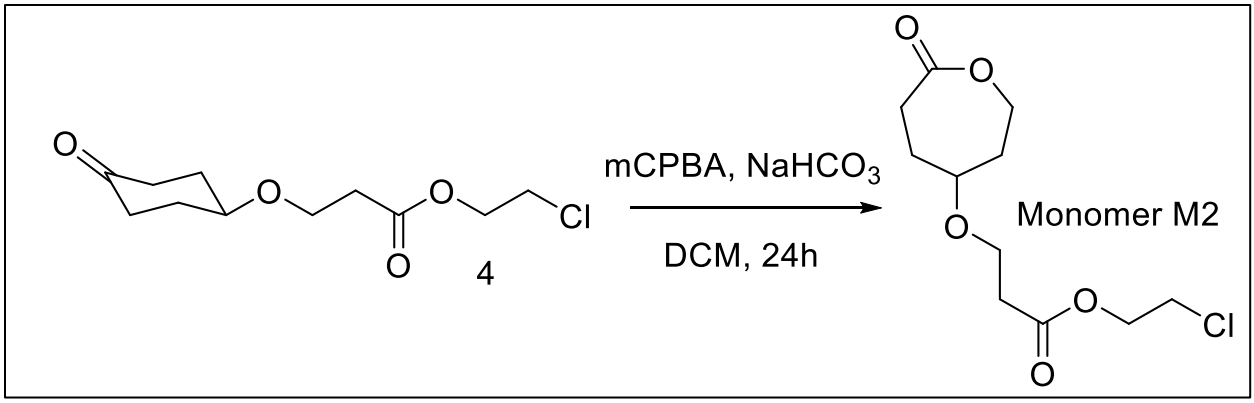

Scheme 2.6

2.3.2 Synthesis of 1-undecyl-1H-imidazole (I11): To the imidazole (3 g, 0.044 mmoles), KOH (4 g, 0.071 mmoles) was added under Nitrogen atmosphere. DMSO (25mL) was added in it, kept for stirring at room temperature. After 1 hour, added 1-Bromoundecane (10 g, 0.0425 mmoles) and kept the reaction mixture overnight at 25℃. Quenched the reaction mixture with H_2O and extraction was done in EtOAc. The organic layer was passed through anhyd. Na2SO4 and solvent was removed to isolate the product. Yield= 8 g (82%).

^{1}H NMR (400 MHz, $CDCl_3$) δ ppm: 7.44 (s, 1H, -CH), 7.02 (s, 1H, -CH), 6.88 (s, 1H, -CH), 3.90 (t, 2H, N-CH_2), 1.75 (m, 2H, N-CH_2-**CH_2**), 1.24-1.28 (m, 16H, -CH_2-), 0.86 (t, 3H, CH_3). ^{13}C NMR (100 MHz, $CDCl_3$) δ ppm: 137.16, 129.43, 118.87, 47.15, 41.11, 32.02, 31.19, 29.65, 29.62, 29.52, 29.39, 29.17, 26.65, 22.72, 14.21.

HRMS (ESI^+): m/z [M +] for $C_{14}H_{26}N_2$ Calculated: 222.2096 and Found:222.1107.

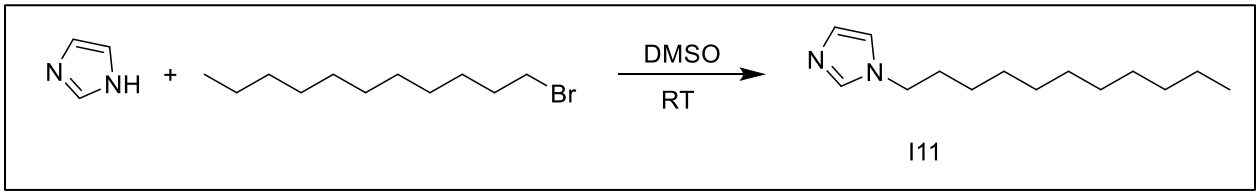

Scheme 2.7

2.3.3 Synthesis of Linear Polymers:

Synthesis of Linear Cationic Polymer (CP1): Triethylene glycol monomethyl ether as initiator was taken for the Ring-Opening Polymerization of Monomer M1. In flame Schlenk tube, initiator (31.8 mg, 0.193 mmoles) was weighed first followed by the addition of Monomer M1 (500mg, 1.93 mmoles). To that, catalyst $Sn(oct)_2$ (39.2 mg, 0.096 mmoles) was added, and High vacuum was applied for 40 min. Then, polymerization setup was kept in a preheated oil bath at 130℃ for 2 h. Cooled it to room temperature, dissolved in 1 mL THF and precipitated in 50 mL Et_2O: Hexane (60:40) mixture at 0℃ to obtain polymer P1. Yield=430 mg (86%).

^{1}H NMR (400 MHz, $CDCl_3$) δ ppm: 4.14 (s, 2H), 3.66 (s, 2H), 3.44 (s, 1H), 3.38 (s, 1H), 2.43 (t, 2 H), 2.37 (t, 2 H), 1.91-1.72 (m, 4H), 1.44 (s, 9H). ^{13}C NMR (100 MHz, CDCl3) δ ppm: 173.49, 170.86, 80.58, 75.46, 64.79, 61.24, 36.47, 32.91, 29.70, 28.90, 28.10. FT-

IR (cm^{-1}): 2965.48, 2926.70, 2870.14,1729.62, 1460.59, 1391.98, 1366.73, 1252.84, 1159.24, 1104.33, 1063.07.847.55.

Further, this polymer P1 was employed as macroinitiator for Ring-Opening Polymerization of Monomer M2. Monomer M2 (300 mg, 1.133 mmoles) was dissolved in Toluene and added to the polymer tube after the addition of P1 (311.3 mg, 0.113 mmoles). To that, $Sn(oct)_2$ (23 mg, 0.056 mmoles) was added, and polymerization was done at 110℃ for 48 h. Precipitation was done in 60 mL Et_2O: Hexane (60:40) mixture at 0℃ to obtain linear diblock polymer P2. Yield=520mg (85%).
^1H NMR (400 MHz, $CDCl_3$) δ ppm: 4.35 (t, 2H), 4.14 (s, 4H), 3.72-3.66 (m, 6H), 3.44 (s, 2H), 3.38 (s, 1H), 2.58 (t,2 H), 2.43 (t, 2 H), 2.37 (t, 4 H), 1.91-1.72 (m, 8H), 1.44 (s, 9H). ^{13}C NMR (100 MHz, CDCl3) δ ppm: 173.30, 170.68, 80.40, 75.45, 64.61, 64.24, 63.96, 61.04, 41.40, 36.29, 34.96, 32.73, 29.52, 28.73, 27.91. FT-IR (cm^{-1}): 2956.78, 2921.45, 2850.90, 1733.26, 1465.21, 1366.49, 1253.92, 1169.70, 1103.62.

Post-modification was done on Polymer P2 (250 mg, 0.46 mmoles), it was taken in a polymerization tube. To that 1-undecyl-1H-imidazole (514 mg, 2.3 mmoles), followed by the addition of 1mL dry DMF. The reaction mixture was kept at 80℃ in oil bath for 72 h. Precipitation was done in Et_2O to get pure cationic diblock polymer CP1. Yield=360 mg (80%)
^1H NMR (400 MHz, $CDCl_3$) δ ppm: 4.75 (s, 1 H), 4.51 (s, 1H), 4.31 (t, 2H), 4.20 (s, 1H), 4.14 (s, 4 H), 3.80 (s, 1H), 3.74-3.62 (m, 5H), 3.45 (s, 2H), 3.37 (s, 1H), 2.58 (t,2 H), 2.45 -2.34 (t, 6 H), 1.89-1.72 (m, 10H), 1.44 (s, 9H), 1.24 (s, 16 H), 0.87 (t, 3H). ^{13}C NMR (100 MHz, CDCl3) δ ppm: 64.58, 61.03, 36.27, 34.92, 32.99, 31.68, 29.33, 29.09, 28.69, 27.88, 26.10, 22.4615.08, 13.91.

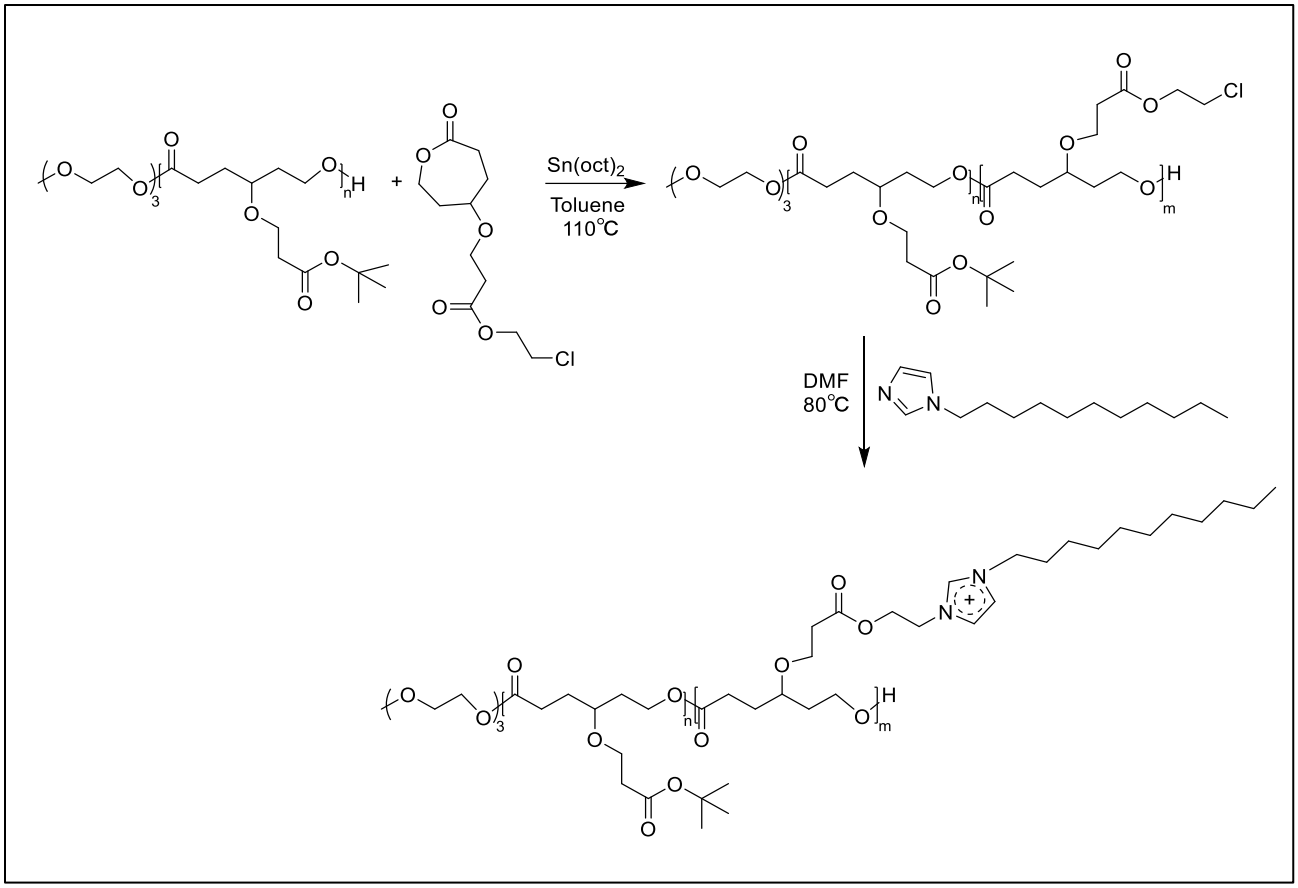

Scheme 2.8

Synthesis of Linear Anionic Polymer (AP1): Triethylene glycol monomethyl ether (31.8 mg, 0.193 mmoles) was weighed and addition of monomer M1 (500 mg, 1.93 mmoles) was done to it. $Sn(oct)_2$ (39.2 mg, 0.096 mmoles) as a catalyst was added and high vacuum was applied for 40 min. Then, reaction is kept at 130℃ in oil bath for 2 hours. Precipitation was done to achieve pure polymer P1. Yield=430 mg (86%). Subsequently, TFA(1.5mL) was added at 0℃ to the polymer (150 mg) dissolved in DCM (2 mL). The reaction mixture was kept for 1 h, and precipitation was then done in Et_20 to obtain anionic Polymer P2. Yield= 110 mg

^{1}H NMR (400 MHz, dmso-D6) δ ppm: 4.04 (s, 2H), 3.56 (s, 2H), 3.50 (s, 1H), 3.23 (s, 1H), 2.39 (t, 2H), 2,32 (t, 2 H), 1.77-1.60 (m, 4H). ^{13}C NMR (100 MHz, DMSO-d6) δ ppm: 173.54, 75.51, 64.87, 61.41, 35.56, 33.01, 29.92, 29.25.

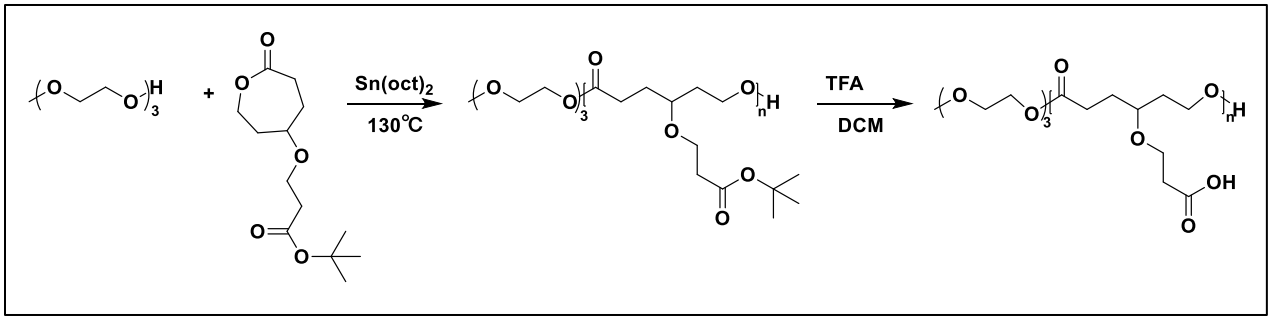

Scheme 2.9

Synthesis of Linear Zwitterionic Polymer (ZP1): Ring-Opening Polymerization was done on monomer M1 (31.8 mg, 0.193 mmoles) using triethlene glycol monomethyl ether (31.8 mg, 0.193 mmoles) as initiator to obtain Polymer P1 (Yield=430 mg). P1 (400 mg, 1.51 mmoles) was further employed as macroinitiator for ROP of monomer M2 (415 mg, 0.151 mmoles) in Dry Toluene (3 mL) to achieve diblock copolymer P2. Subsequently, post-modification was done on polymer P2 (250 mg, 0.46 mmoles) using 1-undecyl-1H-imidazole (514 mg, 2.3 mmoles) in DMF (1 mL) to obtain CP1. The diblock cationic polymer CP1 (150 mg) was then deprotected by the addition of TFA (1.5 mL) at 0℃, reaction was kept at room temperature for 1 h, finally reaction mixture was precipitated in Et_2O to obtain zwitterionic polymer ZP1. Yield=100 mg

^{1}H NMR (400 MHz, dmso-D6) δ ppm: 9.21 (s, 1 H), 7.79-7.68 (m, 2H), 4.47 (s, 1H), 4.39 (s, 1H), 4.26-3.95 (m, 6H), 3.6 (s, 10H), 2.45-2.18 (m, 8H), 1.88-1.60 (m, 8H), 1.26 (s, 16H), 0.87 (s, 3H). ^{13}C NMR (100 MHz, DMSO-d6) δ ppm: 35.56, 31.91, 29.97, 29.60, 29.32, 28.99, 22.72, 14.59

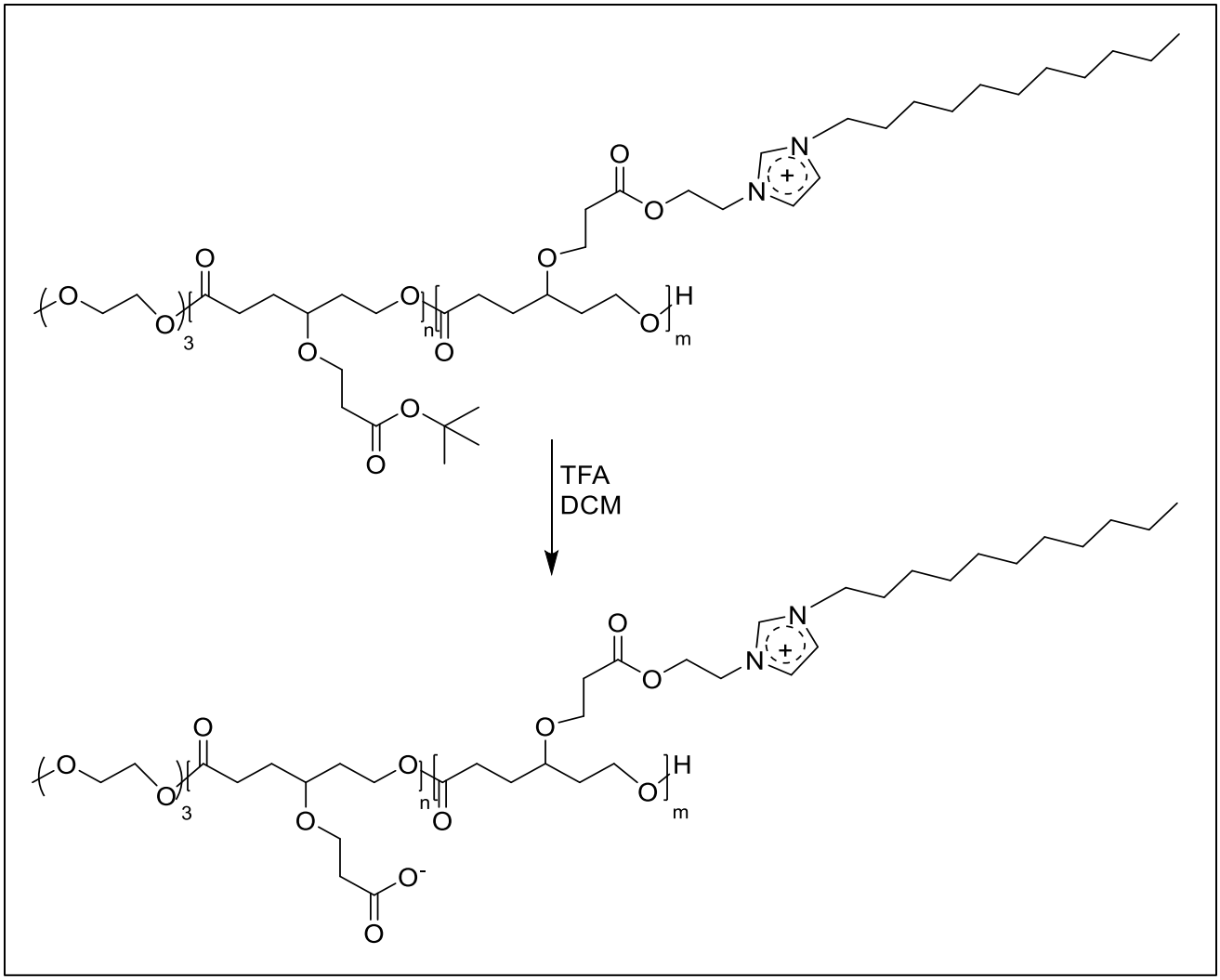

Scheme 2.10

2.3.2 Synthesis of Star Polymers:

Synthesis of Star Cationic Polymer (CP2): To carry out polymerization with a six-arm initiator, custom made melt reactor with an overhead stirrer was builded. To employ polymerization, three equivalence of catalyst and one equivalence of initiator were maintained in the feed ratio. Dipentaerythritol-6-arm initiator (16.4 mg, 0.064 mmoles) was taken in flame Schlenk tube for the Ring-Opening Polymerization of Monomer M1 (1 g, 3.87 mmoles). To that, catalyst $Sn(oct)_2$ (78.4 mg, 0.193 mmoles) was added, and high vacuum was applied for 40 min. Then, polymerization setup was kept at 130℃ for 10 h in a preheated oil bath with constant stirring. Cooled it to room temperature, dissolved in 1mL THF and precipitated in 100 mL Et_2O: Hexane (60:40) mixture at 0℃ to yield pure polymer P3. Yield=900 mg (90%)

^{1}H NMR (400 MHz, $CDCl_3$) δ ppm: 4.14 (s, 2H), 3.66 (s, 2H), 3.44 (s, 1H), 2.43 (t, 2 H), 2.37 (t, 2 H), 1.91-1.72 (m, 4H), 1.44 (s, 9H). ^{13}C NMR (100 MHz, CDCl3) δ ppm: 173.48,

170.85, 80.57, 75.45, 64.80, 61.23, 36.47, 32.92, 29.70, 28.91, 28.10. FT-IR (cm^{-1}): 2966.34, 2922.44, 2850.52,1736.04, 1466.77, 1261.33, 1172.02, 1104.10.

Further, this polymer P3 (402 mg, 0.025 mmoles) was taken as macroinitiator for Ring-Opening Polymerization of Monomer M2. Monomer M2 (400 mg, 1.511 mmoles) was dissolved in Dry Toluene (4mL) and added to the polymer tube after the addition of P3. To that, $Sn(oct)_2$ (31 mg, 0.075 mmoles) was added, and polymerization was done at 110℃ for 48 h. Toluene was removed on rotary vapor and polymer was redissolved in THF (2mL), followed by precipitation in 100 mL Et_2O: Hexane (60:40) mixture to obtain star diblock polymer P4. Yield=710 mg (88%).
^1H NMR (400 MHz, $CDCl_3$) δ ppm: 4.35 (t, 2H), 4.14 (s, 4H), 3.72-3.66 (m, 6H), 3.44 (s, 2H), 2.58 (t,2 H), 2.45 (t, 2 H), 2.36 (t, 4 H), 1.88-1.71 (m, 8H), 1.44 (s, 9H). ^{13}C NMR (100 MHz, CDCl3) δ ppm: 173.49, 170.87, 80.58, 75.46, 64.80, 64.15, 61.23, 41.57, 36.48, 35.14, 31.51, 29.70, 28.84, 28.10, 26.94, 25.22, 22.62, 20.09, 13.93, 11.76. FT-IR (cm^{-1}): 2966.34, 2922.44, 2897.05, 2850.52, 1736.04, 1466.77, 1261.33, 1172.02, 1104.10.

Post-modification was then done, Polymer P2 (250 mg, 0.46 mmoles) was taken in a polymerization tube. To that 1-undecyl-1H-imidazole (520 mg,2.34 mmoles) followed by the addition of 1mL dry DMF. The reaction mixture was kept at 80℃ in oil bath for 72 h. Precipitation was done in Et_2O to get star cationic diblock polymer CP2. Yield= 350 mg (78%).
^1H NMR (400 MHz, $CDCl_3$) δ ppm: 4.76 (s, 1 H), 4.53 (s, 1H), 4.30 (t, 2H), 4.20 (s, 1H), 4.14 (s, 4 H), 3.80 (s, 1H), 3.74-3.62 (m, 5H), 3.44 (s, 2H), 2.58 (t, 2 H), 2.45 -2.34 (t, 6 H), 1.90-1.69 (m, 10H), 1.44 (s, 9H), 1.24 (s, 16 H), 0.87 (t, 3H). ^{13}C NMR (100 MHz, CDCl3) δ ppm: 64.79, 61.24, 36.48, 32.77, 31.88, 29.29, 28.10, 26.31, 22.67, 14.11.

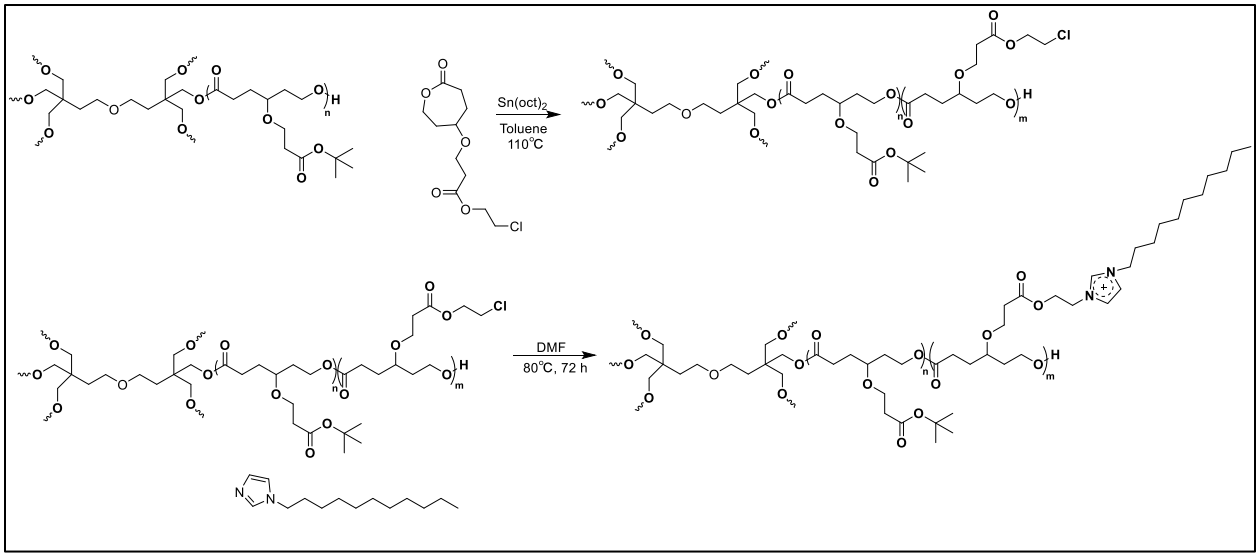

Scheme 2.11

Synthesis of Star Anionic Polymer (AP2): Dipentaerythritol (16.4 mg, 0.064 mmoles) was used as initiator for Ring-Opening Polymerization of monomer M1 (1 g, 3.87 mmoles) in the presence of catalyst $Sn(oct)_2$ (78.4 mg, 0.193 mmoles) at 130℃ for 10 h, followed by precipitation to obtain pure polymer P1. To polymer P1 (150 mg) dissolved in DCM, TFA(1.5 mL) was added at 0℃. The reaction mixture was kept for 1h, and precipitation was then done in Et_2O to obtain star anionic Polymer AP2. Yield= 100 mg
^{1}H NMR (400 MHz, dmso-D6) δ ppm: 4.03 (s, 2H), 3.56 (s, 2H), 3.40 (s, 1H), 2.38 (t, 2H), 2,31 (t, 2 H), 1.77-1.60 (m, 4H). ^{13}C NMR (100 MHz, CDCl3) δ ppm: 172.90, 74.86, 64.22, 60.77, 34.92, 32.50, 28.60.

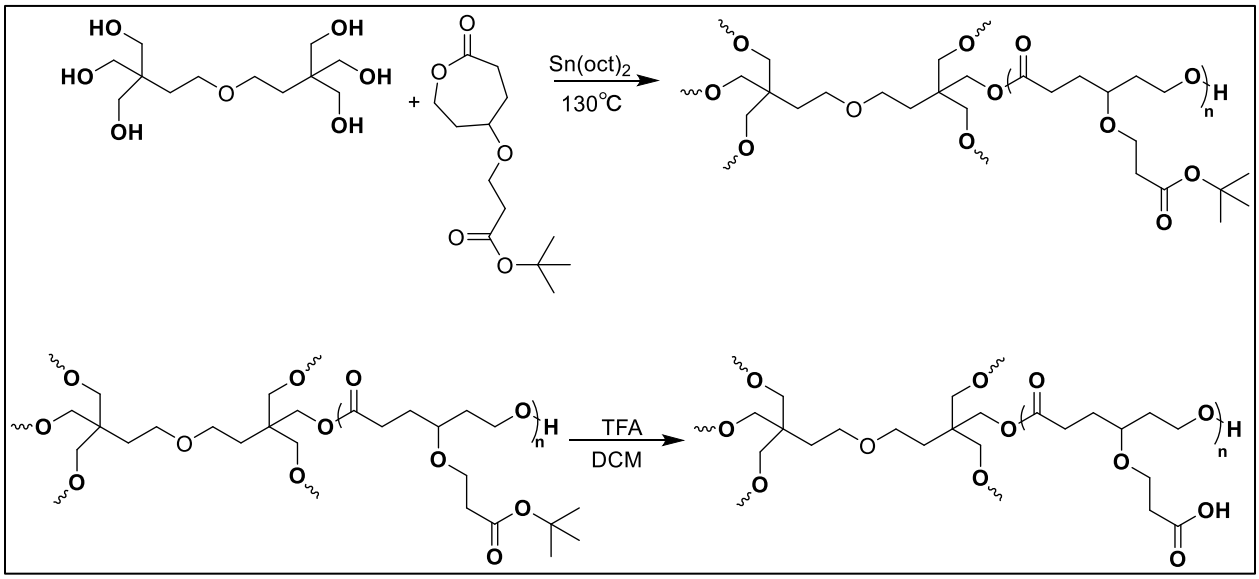

Scheme 2.12

Synthesis of Star Zwitterionic Polymer (ZW2): Ring-Opening Polymerization was done on monomer M1 (1 g, 3.87 mmoles) using 6-arm initiator Dipentaerythritol (16.4 mg, 0.064 mmoles) to obtain Polymer P1, which was further employed as macroinitiator (402 mg, 0.025 mmoles) for ROP of monomer M2 (400 mg, 1.511 mmoles) to achieve star diblock copolymer P2. Subsequently, post-modification was done on P2 (250 mg, 0.46 mmoles) using 1-undecyl-1H-imidazole (520 mg,2.34 mmoles) to obtain star diblock cationic polymer CP1. The polymer CP1 (150 mg) was then deprotected by the addition of TFA (1.5mL) at cold conditions and kept the reaction mixture for 1 h, followed by precipitation in Et_2O to obtain star zwitterionic polymer ZW2.
^{1}H NMR (400 MHz, dmso-D6) δ ppm: 9.14 (s, 1 H), 7.78-7.70 (m, 2H), 4.47 (s, 1H), 4.39 (s, 1H), 4.19 (t, 2H), 4.05 (m, 4H), 3.60-3.30 (m, 8H), 2.42-2.25 (m, 8H), 1.88-1.57 (m, 8H), 1.23 (s, 16H), 0.87 (s, 3H). ^{13}C NMR (100 MHz, CDCl3) δ ppm: 122.45, 120.41, 31.75, 29.86, 25.99, 22.55, 14.42.

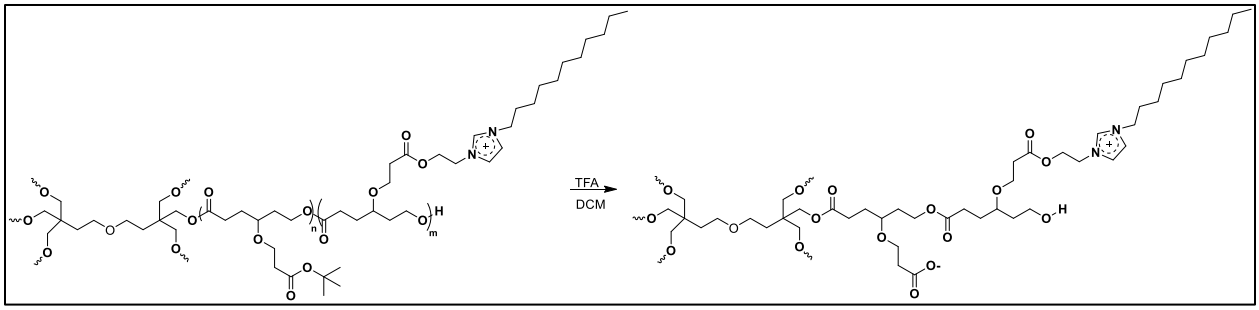

Scheme 2.13

2.3.4 Self- assembly of Polymers:

For all the polymers, the same procedure was followed for self-assembly. 5 mg of polymer sample was dissolved in 0.6 mL DMSO. To a small vial containing 4.4 mL Milli-Q H_2O, added polymer solution dropwise for 15-20 minutes. Kept on stirring at room temperature for 4 hours. Then, transferred the solution to dialysis tube (MWC0= 1000 Da) and dialyzed it against water. The water was recharged at a regular interval for 24 hours water to ensure complete removal of DMSO.

2.3.5 pH dependent studies of Polymers:

10 vials of each containing 200 µL of dialyzed solution of polymer, to that 50 µL of pH buffer of range: 2.7, 3.9, 4.8, 5.7, 6.7, 7.4, 8.64, 9.85, 11.08, 12.68 was added in each vial and labelled. Then, diluted each sample with 750 µL Mili-Q water to make overall 1 mL solution. Further, DLS and Zeta Potential were measured for all the pH range. Similar protocol was followed for pH dependent study of all the polymers.

2.3.6 Dye encapsulation in the Zwitterionic Polymers:

To the polymer 5 mg dissolved in 600 µL DMSO, 0.5 mg of anionic dye 8-hydroxypyrene-1,3,6-trisulfonic acid trisodium salt (HPTS) in 200 µL was added. To a vial containing 4.2 mL of Mili-Q H_2O, overall polymer solution with HPTS dye was added very slowly for 20 minutes and covered the vial with aluminum foil. Stirred it at 25℃ for 4 hours. Transferred it to dialysis tube (MWC0=1000 Da), dialyzed against Mili-Q water for 24 hours by recharging the water at a regular interval to remove the unencapsulated dye and DMSO. Using, UV-visible spectroscopy, Drug loading efficiency (DLE) and Drug loading content (DLE) were calculated using the following equations:

$$\textbf{DLC \%} = \textbf{[Weight of encapsulated HPTS /Weight of polymer]} \times \textbf{100}$$

$$\textbf{DLE \%} = \textbf{[Weight of encapsulated HPTS /Weight of HPTS in the feed]} \times \textbf{100}$$

Chapter 3 Results and Discussion

3.1 Synthesis and Characterization of γ-substituted Monomers:

The designing of two γ-substituted caprolactone monomer have been done using multistep synthesis. Michael addition was done on 1,4 cyclohexanediol by treating it with t-butyl acrylate, isolated monosubstituted product **1**, which on further oxidation with PCC yielded t-butyl substituted cyclohexanone derivative **2.** Monomer **M1** was synthesized by Baeyer-Villiger Oxidation on Compound **2**. The presence of **Hb** protons in compound **1** as separate peak was observed due to the presence of cis-trans mixture in the 1,4 cyclohexanediol. Further, in compound **2**, this peak vanished. Finally, the synthesis of monomer M1 was determined by the peaks corresponding to 7-membered caprolactone ring marked as **a, b, c, d, e.**

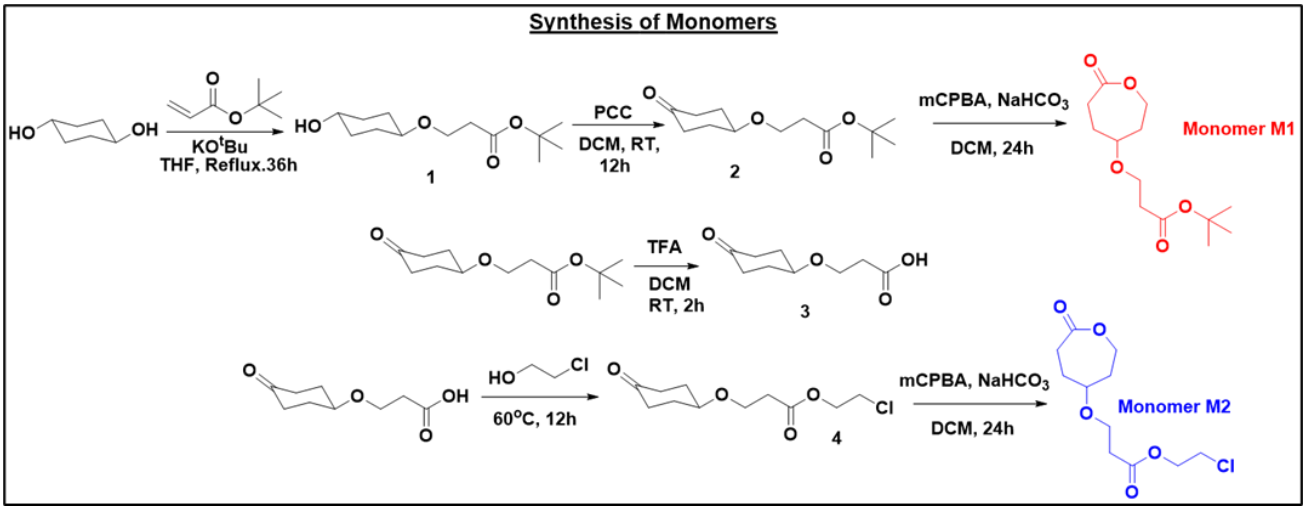

Fig 3.1 Monomer synthesis scheme

To synthesize Monomer **M2**, compound **2** was deprotected, further coupled with chloroethanol, finally on Baeyer-Villiger oxidation chlorine substituted Monomer **M2** was fabricated. The deprotection was confirmed by the disappearance of proton e in compound **3**. Further, coupling with chloroethanol was observed due to the appearance of new peaks **a, c** in compound **4**. Further **M2** monomer synthesis was monitored by the caprolactone protons. All the steps involved in the monomer synthesis were characterized by ^{1}H NMR, ^{13}C NMR, FT-IR and HRMS.

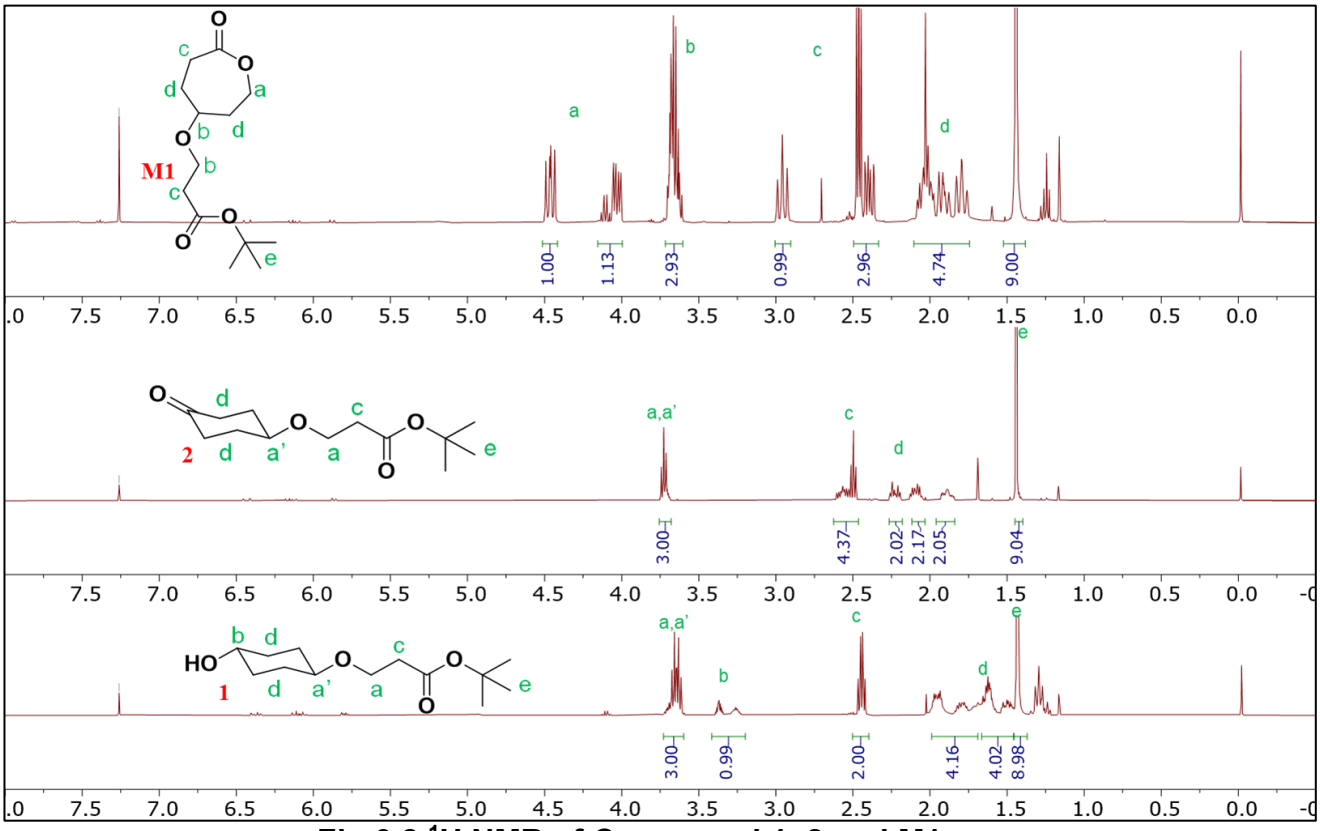

Fig 3.2 ^{1}H NMR of Compound 1, 2 and M1

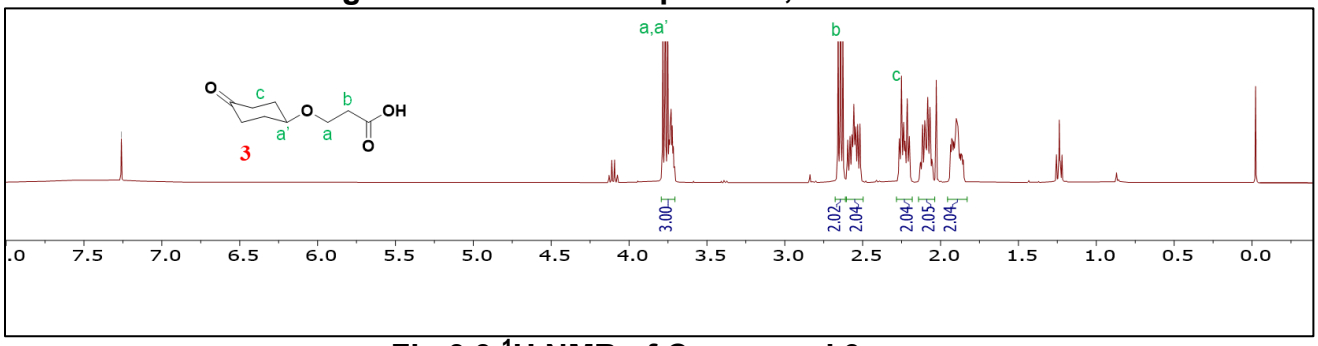

Fig 3.3 ^{1}H NMR of Compound 3

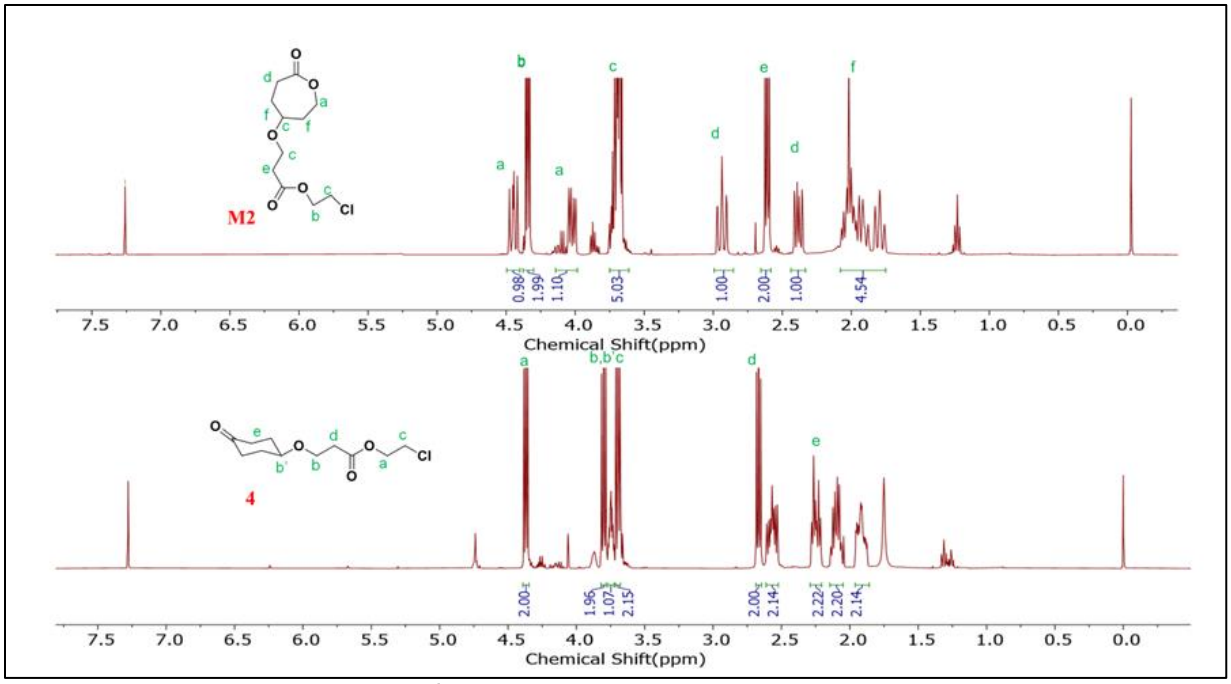

Fig 3.4 ^{1}H NMR of Compound 4 and M2

3.2 Synthesis and Characterization of 1-undecyl-1H-imidazole:

The synthesis of 1-undecyl-1H-imidazole was done using imidazole in the presence of base KOH, which reacted with 1-Bromoundecane. It is characterized by 1H NMR, due to the presence of imidazole peaks **a, b, c** and alkylated chain protons **d, e, f, g.** Further, this compound I-11 was characterized using 13 C NMR, FT-IR.

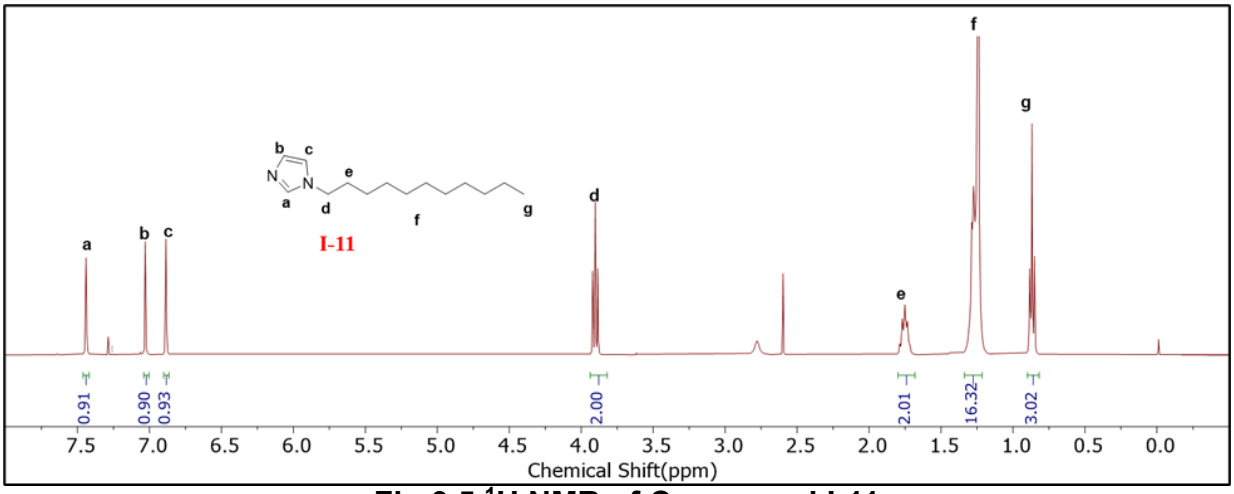

Fig 3.5 ^{1}H NMR of Compound I-11

3.3 Synthesis and Characterization of Linear Polymers:

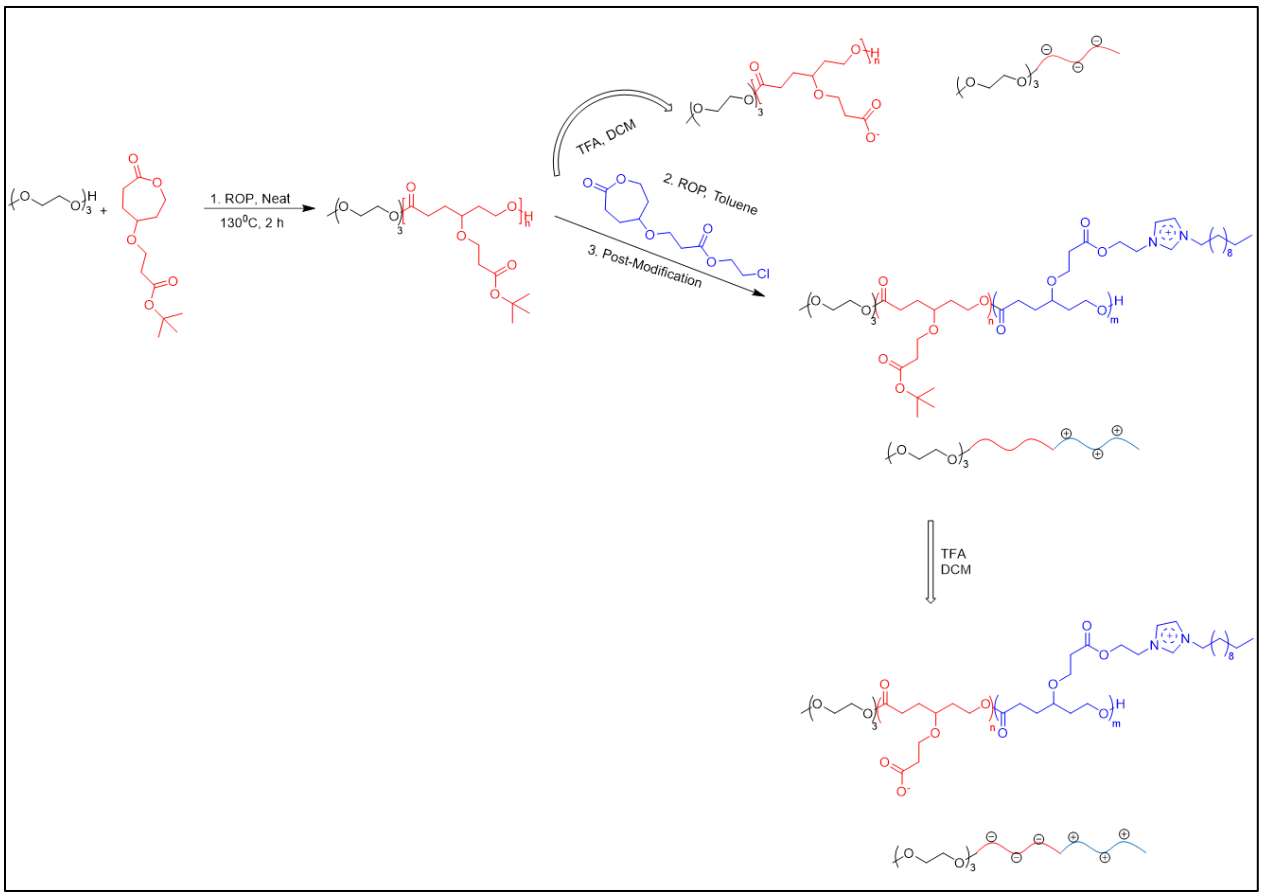

Fig 3.6 Reaction Scheme of Linear Polymers

For Ring-Opening Polymerization, the degree of Polymerization was calculated by comparing initiator protons with respect to the polymer protons. Characterization of Linear Homopolymer **P1** was done by monitoring the **-CH3** proton of initiator at 3.38 ppm for 3H, with respect to a proton corresponding to 2H in the polymer backbone, which confirmed the formation of 10 unit.

Further, this polymer **P1** was employed as macroinitiator for Ring-Opening Polymerization of chlorine substituted monomer **M2** to give diblock monomer. Further, P' proton corresponds to 2H, confirmed the incorporation of 11 units of second block in the polymer P2. Further, the post-modification to obtain cationic polymer **CP1** formation was confirmed by monitoring protons **P, Q** that ensured complete quaternization.

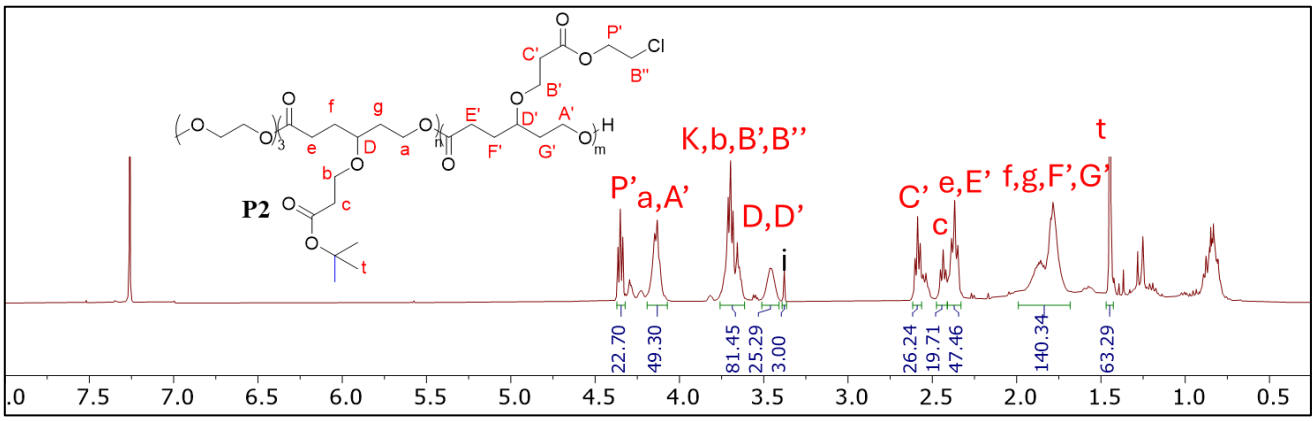

Fig 3.7 ^{1}H NMR of Linear Homopolymer P1

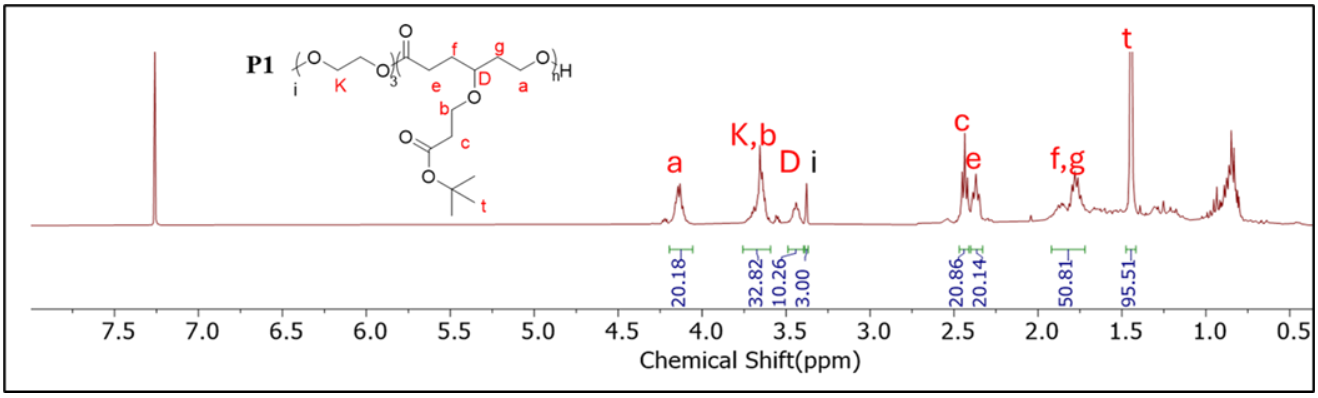

Fig 3.8 ^{1}H NMR of Linear Block copolymer P2

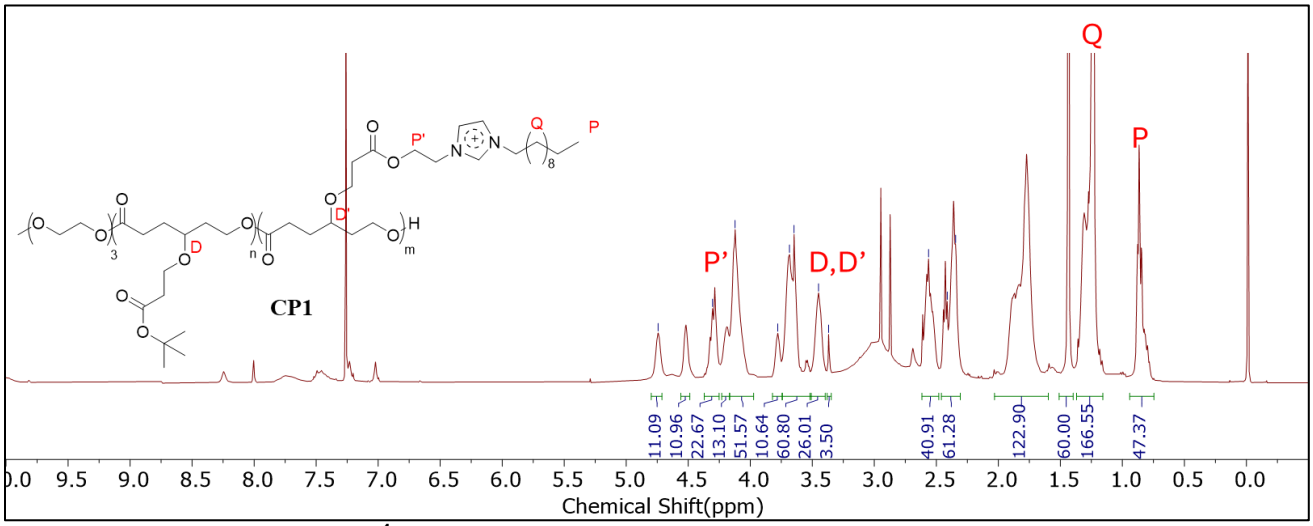

Fig 3.9 ^{1}H NMR of Linear Cationic Polymer CP1

Further, deprotection of Polymer P1 was done to get anionic polymer **AP1**, which was monitored by the vanishing of t-butyl peak in the ^{1}H NMR.

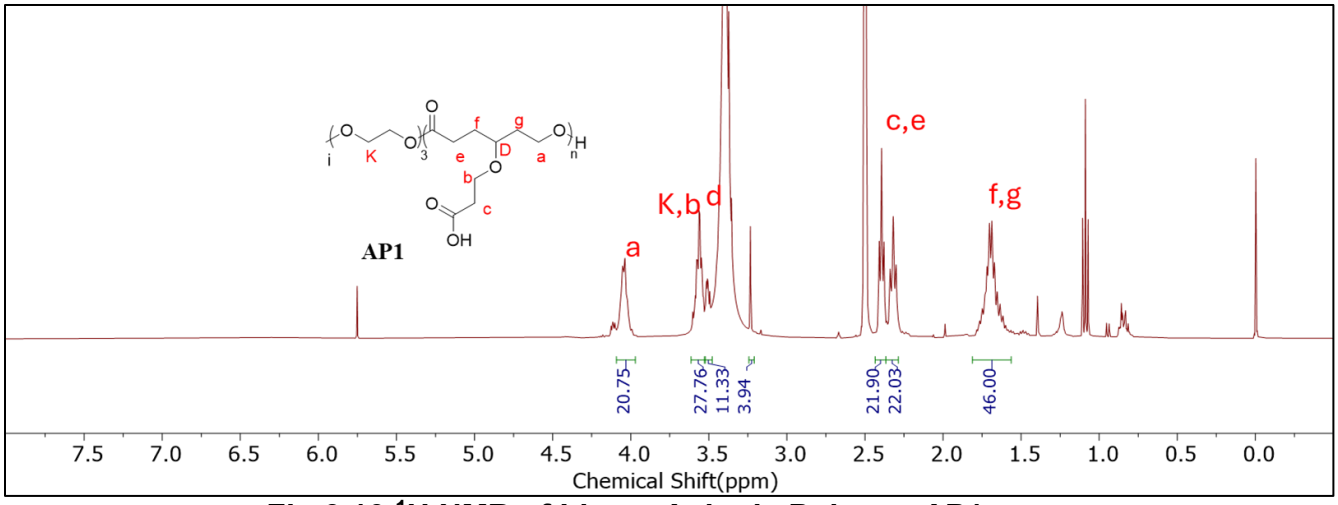

Fig 3.10 ^{1}H NMR of Linear Anionic Polymer AP1

The zwitterionic polymer **ZP1** was employed by the deprotection of polymer **CP1**, confirmed by the vanishing of t-butyl peaks, and here the protons corresponding to imidazole units **A, B, C** were also visible.

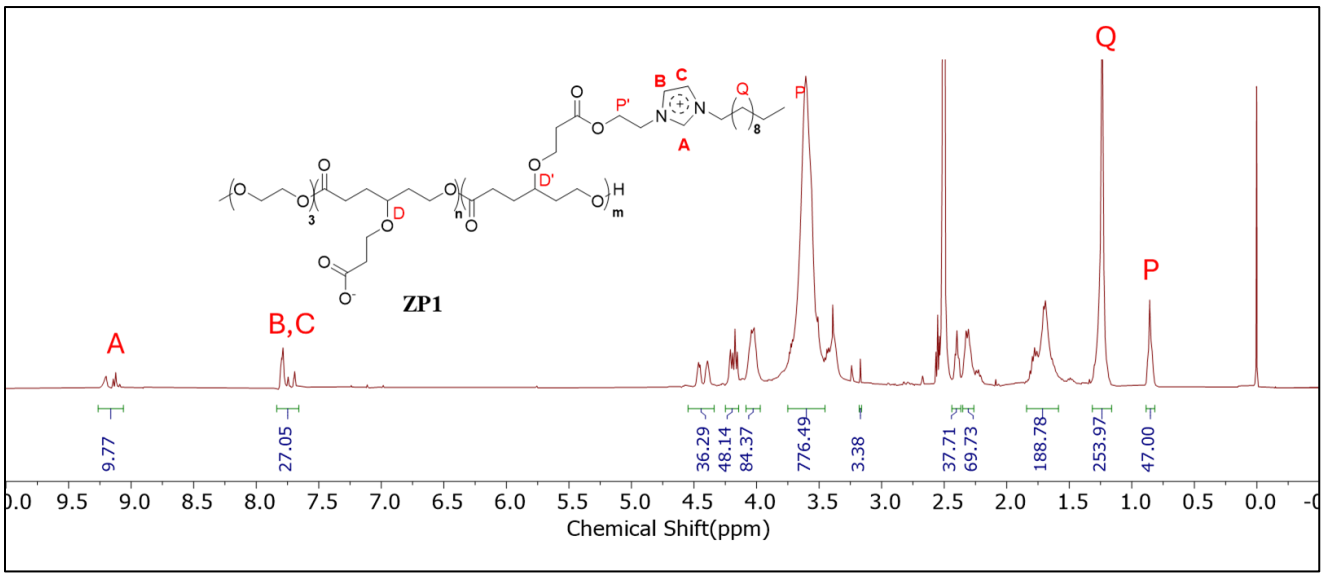

Fig 3.11 ^{1}H NMR of Linear Zwitterionic Polymer ZP1

3.4 Synthesis and Characterization of Star Polymer:

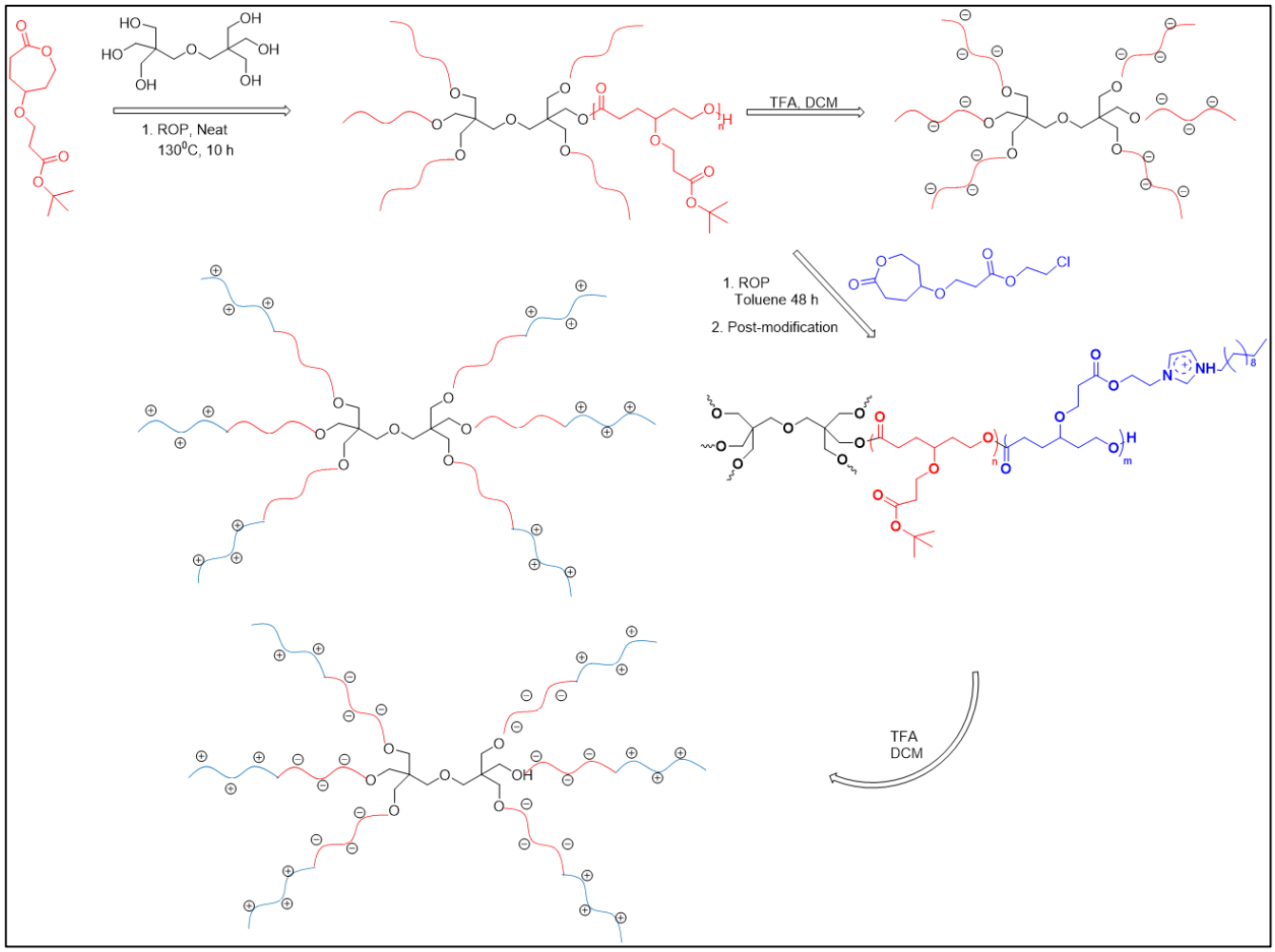

Fig. 3.12 Reaction Scheme of Star Polymers

Six-arm initiator, dipentaerythritol, was employed as initiator for Ring-Opening Polymerization of t-butyl substituted monomer M1 in the presence of $Sn(oct)_2$ as a catalyst in a specially designed overhead melt reactor. Degree of Polymerization was calculated by monitoring the dipentaerythritol initiator, 4 ether protons **(K)** at 3.39 ppm with polymer peak **D** as they appeared together, they were integrated as 64 (reference peak, feed ratio was kept as [M]/[I]=60). The newly formed ester peak appeared at 4.10, 3.65, 2.35, 2.43 ppm. As 12 protons **(i)**, corresponding to initiator came around 4.06 ppm with proton **a**. To find the incorporated degree of polymerization (Xn), compared the intensities of **a, i** with the reference, which confirmed the incorporation of 60 units in the polymer **P3**, 10 units statistically on each arm. Also, the end group protons for 12 H came together with proton **b** at 3.65. Subsequently, this polymer was used as macroinitiator for Ring-Opening Polymerization of chlorine substituted monomer M2 in $Sn(oct)_2$ and toluene. To estimate the degree of polymerization in polymer **P4**, the appearance of new peak **P'**, was

compared with the macroinitiator. As the new peak **D'** also merged with the earlier protons **K,D**; so together they were integrated as 130 (here also feed ratio was maintained as [M]/[I]=600). Finally, the incorporation of 60 units of second block in the polymer backbone was confirmed using ^{1}H NMR. Further, the synthesis of cationic star polymer **CP2** was done by the post-modification of the diblock polymer **P4** with 1-undecyl-1H-imidazole**.** The appearance of new peaks **P,Q** confirmed the complete quaternization in the diblock polymer.

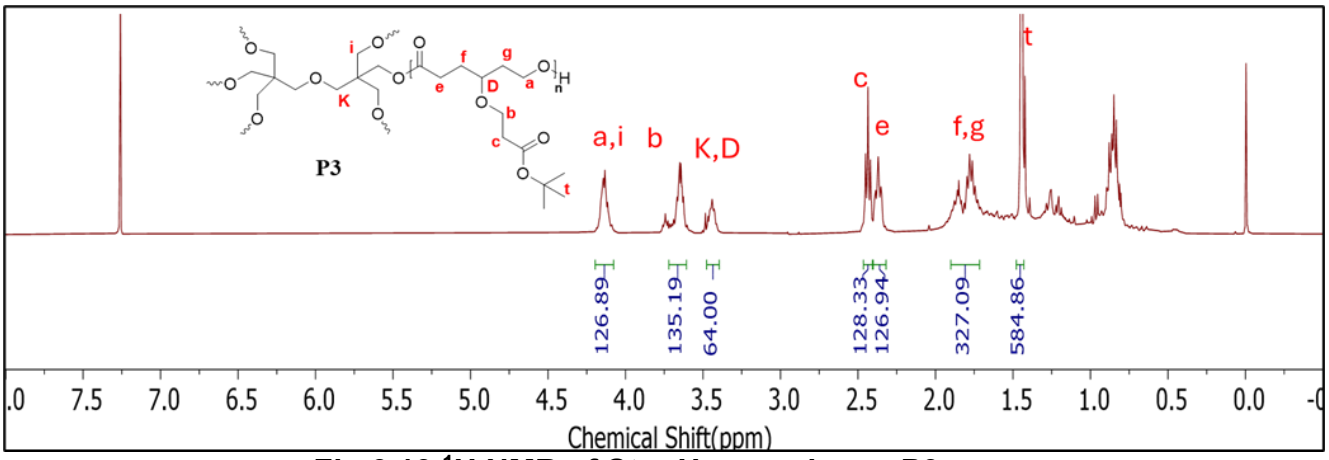

Fig 3.13 ^{1}H NMR of Star Homopolymer P3

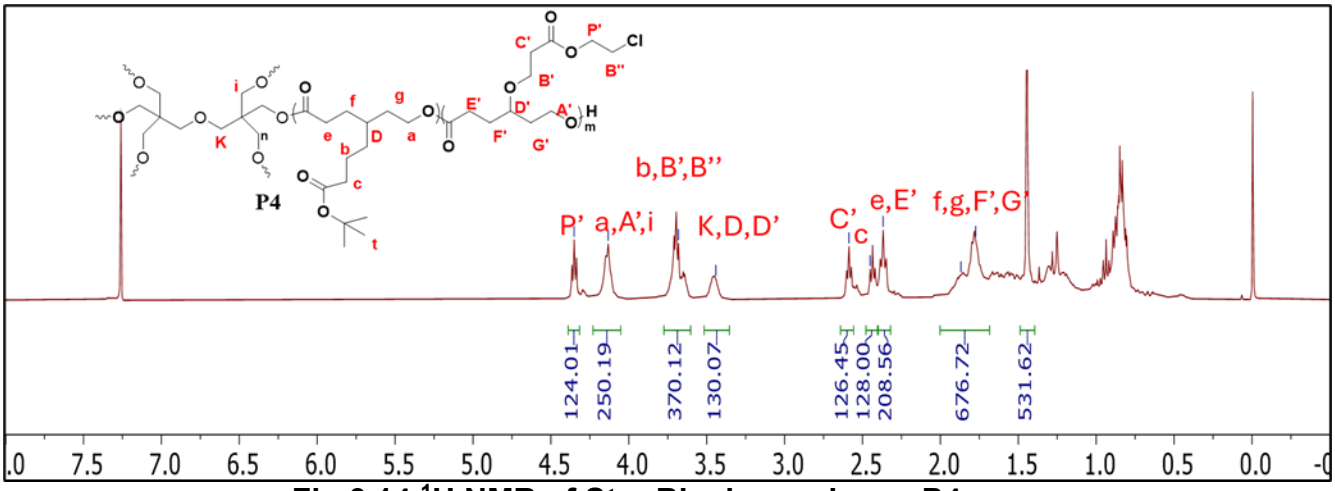

Fig 3.14 ^{1}H NMR of Star Block copolymer P4

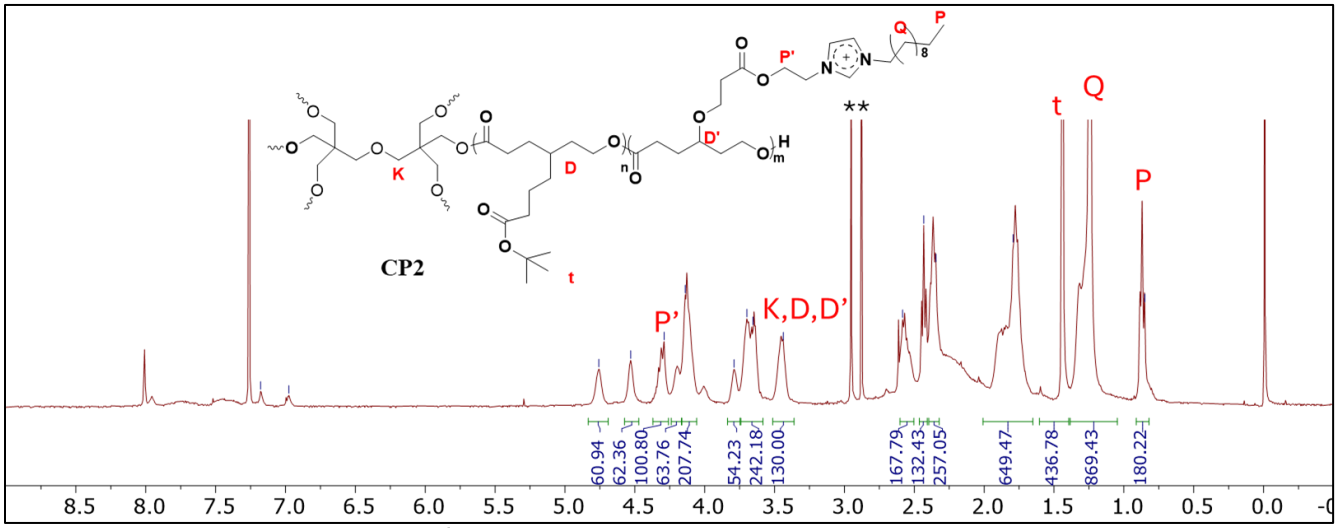

Fig 3.15 ^{1}H NMR of Star Cationic Polymer

The deprotection was done using TFA on polymer P3 to achieve star anionic polymer AP2, which was monitored by the vanishing of t-butyl peaks.

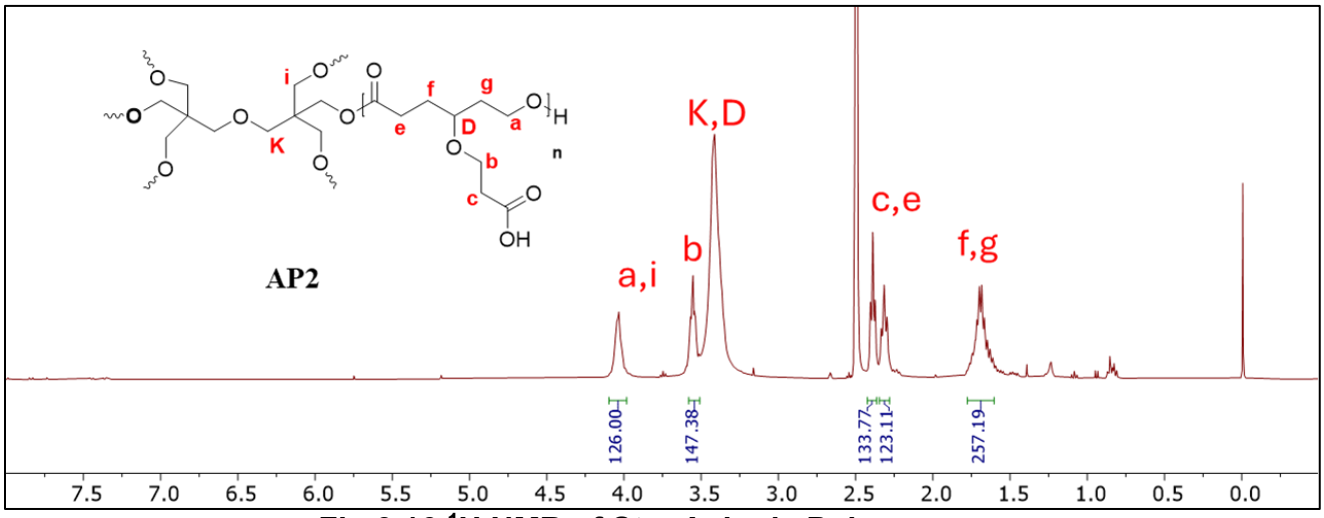

Fig 3.16 ^{1}H NMR of Star Anionic Polymer

Further, the deprotection of polymer CP1 was done to employ zwitterionic polymer ZP2, confirmed by the disappearance of t-butyl peaks and appearance of imidazole protons A, B, C in the final step of NMR.

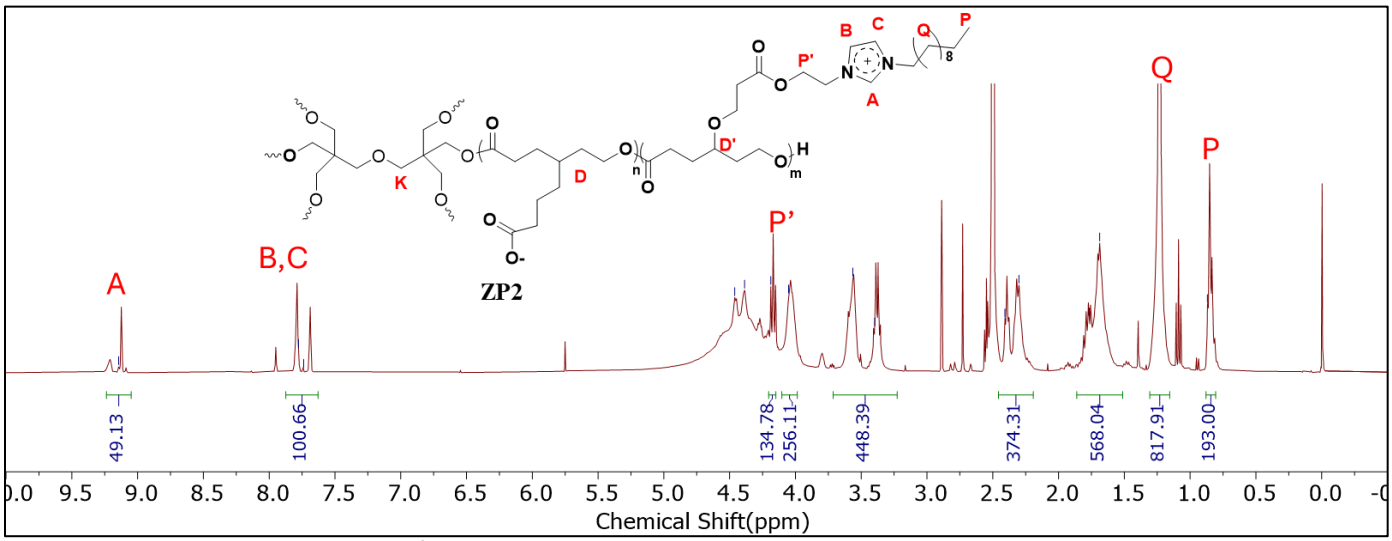

Fig 3.17 ^{1}H NMR of Star Zwitterionic Polymer

3.5 Molecular weight estimation and Thermal stability of Polymers:

The molecular weights of the newly synthesized linear and star homo polymer and diblock polymers were analyzed using gel permeation chromatography (GPC) using polystyrene as standard in CHCl3 as a solvent. Both the homopolymer and diblock polymer showed monomodal distribution and their corresponding Mn, Mw, and polydispersity index (Mw/Mn) were summarized in table 1. In the case of linear polymers, it was clearly observed that higher molecular weight diblock polymer elutes first than linear homopolymer. But for the case of star polymer, both the homopolymer and star diblock elutes almost at the same time. This may be attributed to the small hydrodynamic volume in the case of star polymers which was not differentiated by using polystyrene standard. Due to the limited facility of mobile phases in GPC systems, unable to record the chromatograms for charged polymers. Because charged polymers showed restricted solubility for solvents (soluble in DMSO).

Entry	Polymers	M_n NMR (g/mol)	M_n SEC (g/mol)	M_w SEC (g/mol)	Đ	Tg (°C)
1	LN-BPCL$_{10}$	2700	2000	2800	1.3	-22.2
2	LN-BPCL$_{10}$-b-Cl$_{10}$	5400	4100	7100	1.7	-30.7
3	ST-BPCL$_{60}$	16000	12000	18000	1.5	33.9
4	ST-BPCL$_{60}$-b-Cl$_{60}$	32000	21000	39000	1.7	-22.9

Table 1: Molecular weight and thermal properties of Polymers

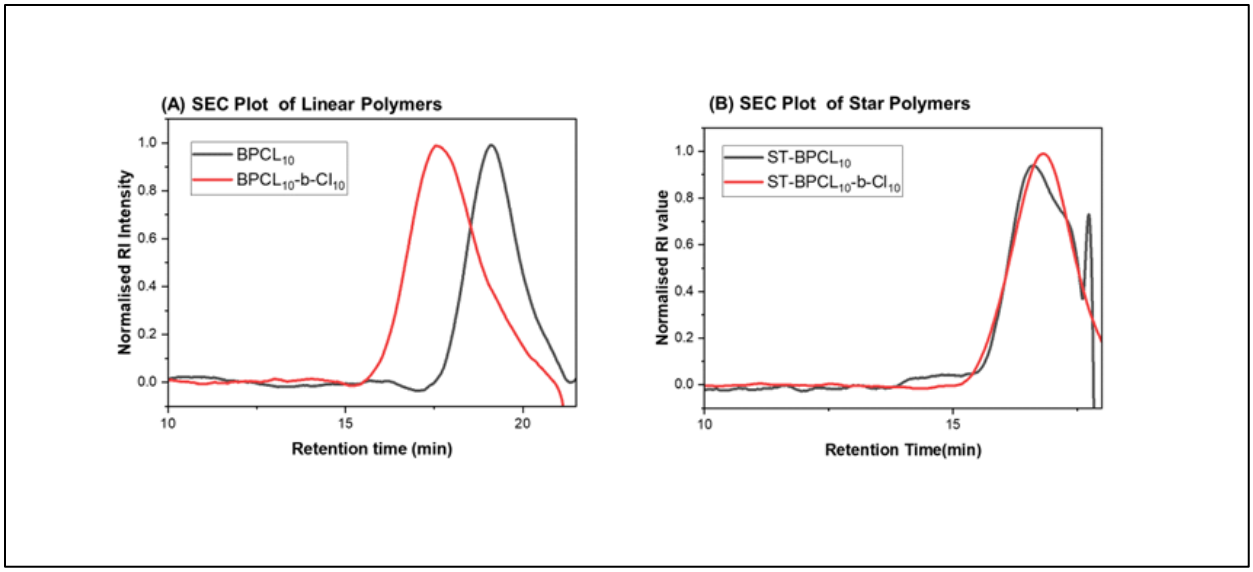

Fig 3.18 SEC plots for Linear and Star Polymers

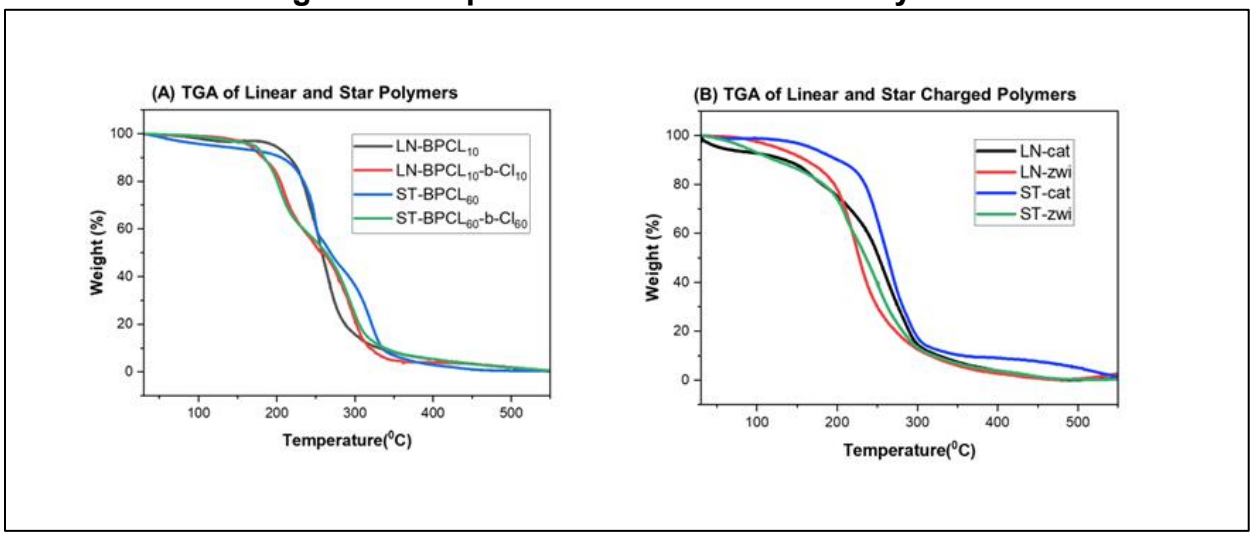

Fig 3.19 Thermogravimetric analysis of Uncharged and Charged polymers

The underestimation of molecular weights was observed in GPC comparative to their calculated Mn from NMR, due to the limitation of calibration standard, polystyrene. The PDI observed for diblock polymers came to 1.7, while for homopolymers it was observed to be in the range of 1.3-1.5. The PDI reports showed little deviation as compared to PCL, it was expected for substituted PCL from our earlier reports. Hence, it may be concluded that the development of new class of linear and star diblock polymers are good to fabricate controlled molecular weight using ROP process. Thermal stability of linear and star homopolymer and diblock polymers were monitored using thermogravimetric analysis (TGA) under Nitrogen at 10°C/min. It was observed that homopolymer in both the cases were more stable as compared to their respective diblock polymers. Also, the TGA analysis of cationic and zwitterionic polymer showed that they are less stable than the uncharged polymers.

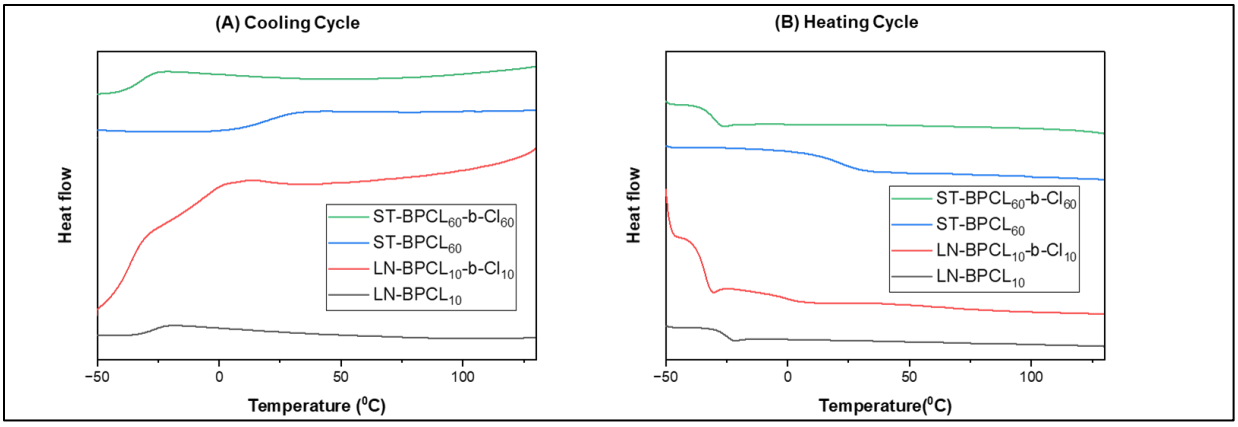

Fig 3.20 DSC thermograms of Linear and Star Polymers

To examine the crystalline and amorphous nature of the homo and block copolymers, Differential scanning calorimetry was carried out. All the polymers were found to be amorphous in nature due to the presence of substituted backbone introducing steric hindrance and disrupting the crystallinity of PCL backbone. The glass transition temperature was obtained in the range of -22℃ to -30℃ for linear substituted caprolactone polymers and 34℃ to -22℃ for substituted star polymers.

3.6 Self-assemblies of charged polymer nanoparticles:

The designing of newly synthesized amphiphilic polymers due to the presence of hydrophobic backbone and charged groups as hydrophilic pendant groups in the repeating units showed the polymer ability to self-assemble in water.

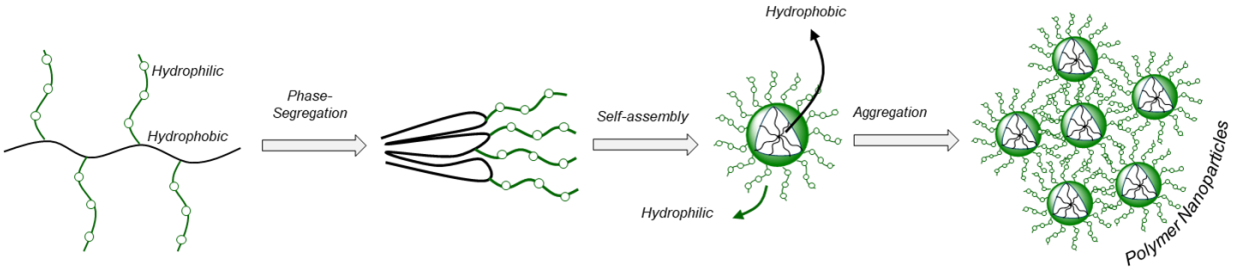

Fig 3.21 Self-assembly in Polymer backbone

To determine their self-assembly studies, polymer nanoparticles were subjected to Dynamic Light Scattering (DLS) and Zeta Potential measurements.

The size of polymer nanoassemblies are shown by DLS histograms in Fig **3.22**. The size corresponding to star polymers in all the cases were found to be smaller than the linear polymers. This was attributed to the small hydrodynamic volume and topology of star polymers contributing to the smaller size of charged polymeric nanoparticles. The three-

dimensional network of star polymers introduces chain collapsing, thus minimizing its overall sizes.

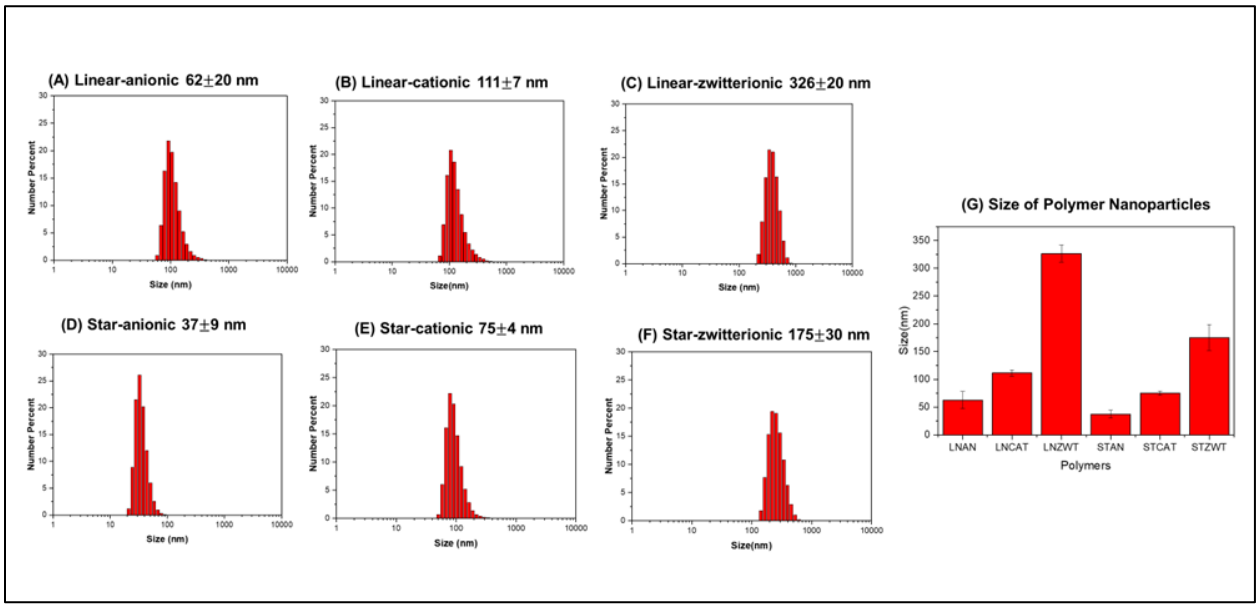

Fig 3.22 Nanoparticle characterization using DLS

The charges on polymer nanoparticles were examined using zeta potential studies, shown in Fig **3.23**. Also, the studies of zeta potential confirmed the presence of positive and negative charges in the cationic and anionic nano-scaffolds. While in the case of zwitterionic nanoparticles, they were found to be of negative charge. This may be attributed due to the more effect of deprotected core in the zwitterionic moieties, while the delocalization of positive charges in the imidazole pendant units ultimately reducing its overall effect. So, overall, the negatively charged core of the zwitterionic nanoparticles dominates over the delocalized positive charge. This could be the possible reason for zwitterionic moiety to not showing net zero charge.

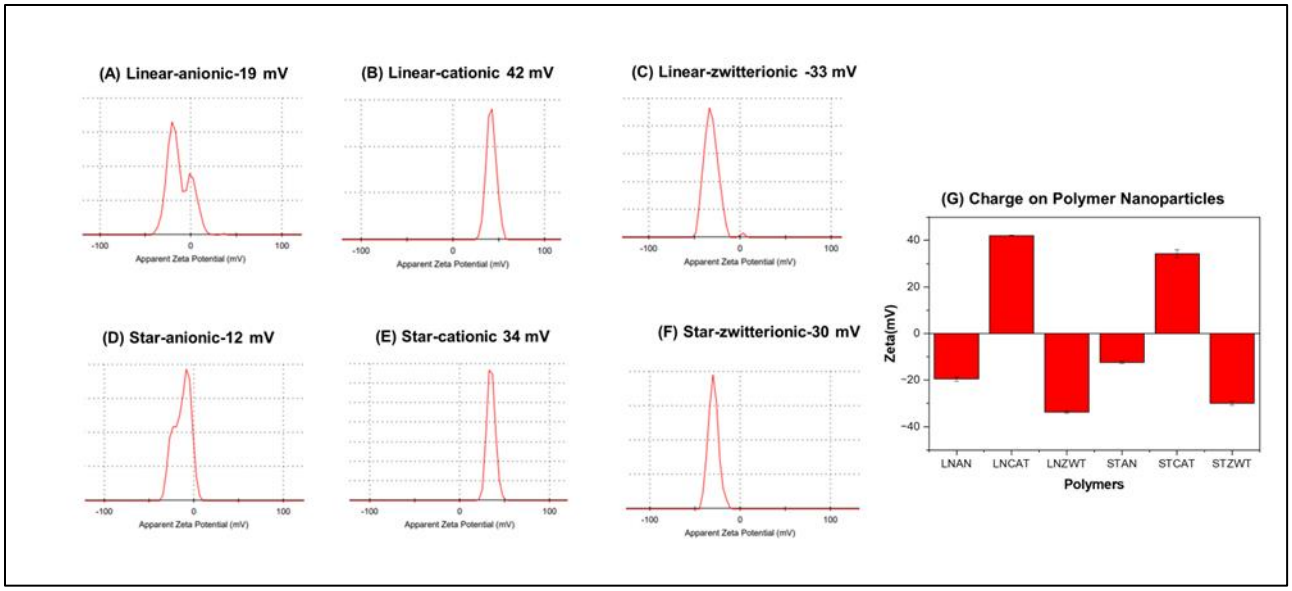

Fig 3.23 Nanoparticle characterization using Zeta Potential

3.7 pH dependent studies for charged polymers:

The electrically charged polymer nanoparticles showed significant changes in the solution with the changes in pH. These charged species tend to move under the effect of electric field, which was monitored by employing Zeta potential measurements. Also, the stability and size of nano-assemblies were confirmed by the DLS studies with variation in pH. Size and zeta potentials were plotted as a function of pH for the linear and star charged assemblies in **Fig 3.24 and Fig 3.25.**

For linear and star anionic, sizes observed are high at initial pH. Gradual decrease in size observed as pH increases, confirming the stability of negatively charged nanoparticles. At pH=2.7, star anionic shows higher size compared to its corresponding linear nanoparticles. This could be attributed to the higher shielding and charge instability in acidic range. At pH=5.7, both the anionic polymers inhibit the same size and further remain stable at all pH ranges, despite the presence of a greater number of repeating units in the star polymers. This clearly depicts the role of star topology in altering the overall three-dimensional macro-structures. The role of engineering linear and star polymers alters the property of polymers effectively by modification of their hydrodynamic volume.

Further, in the case of cationic polymers, star polymer shows lower sizes from pH=2.7 itself, confirming its stability and the chain collapsing of the diblock cationic copolymer resulting in the smaller sizes. Here, the presence of more cationic units in star polymers effectively resulted in chain collapsing, thus overall changes the size characteristics. As the pH, corresponds to basic range, both the nanoparticles inhibit the stable nature, but at higher pH range of 12.68, both the nano-scaffolds confirms the introduction of instability in the polymer backbone. This deviation is observed more for star polymers due to the more disruptions happening in the star polymer core-shell structure.

Finally, in the case of zwitterionic polymers, a contrast between the sizes of linear and star polymers has been observed. In the case of linear zwitterionic polymers, sizes are almost same in acidic range up to pH=4.8. At pH=5.7, sudden increase in size was observed, and after that it almost remains constant, confirmed the stable zwitterionic nanoparticles. While in the case of star zwitterionic nano-scaffolds, the nanoparticles are not that much stable, as at pH=4.8 sharp increase is observed and further decay in sizes to the pH=6.7, further size increases to the pH=8.64, and finally it shows stable nanoparticle behavior. This is due to the charge imbalance dominating in the case of star polymers, while it is easily neutralized in the case of linear polymers. This shows the topology of polymers making an overall control on the charge balancing and stability of macro-architectures to display zwitterionic characters.

To examine the charge characters, zeta potential measurements have been done. For anionic polymers, at pH=2.7, the overall effect of the core in the star polymer backbone introduces nearly negligible positive charge while for the case of linear anionic polymers, the overall positive charge is higher. As the pH increases further, the dominance of negatively charged character appears for both the cases, both the nanoparticles exhibit negative charges at all pH ranges, but the overall negative charges increment is observed in basic pH values.

For cationic polymers, star cationic polymers show an overall positive charge from pH=2.7 to 11.08, which decreases gradually with pH, but at the highest pH range of 12.68, cationic nanoparticles demonstrate the negative characters. The net role of star core is contributing the positive charge, in pH dependent studies, confirms the positive feature of polymer nano-scaffolds. While in the case of linear cationic polymers, positive nature is clearly visible in acidic range, as the pH moves to basic around 8.64, nearly neutral behavior has been observed, which continues till the pH value of 12.68.

In the zwitterionic scaffolds, typical characteristics of zwitterionic nanoparticles have been seen. The change in the charge from positive to negative, via showing the overall zero charge and maintain electroneutrality around pH=6 for linear zwitterionic polymers, while the same observation is depicted by the star zwitterionic nanoparticles around pH=5, shows the zwitterionic characteristics of the nanoparticles. And the deviations are observed from pH=8.64 onwards in the star zwitterionic scaffolds. This could be attributed to the effective imbalance of charges in the basic pH values in the star nanoparticles.

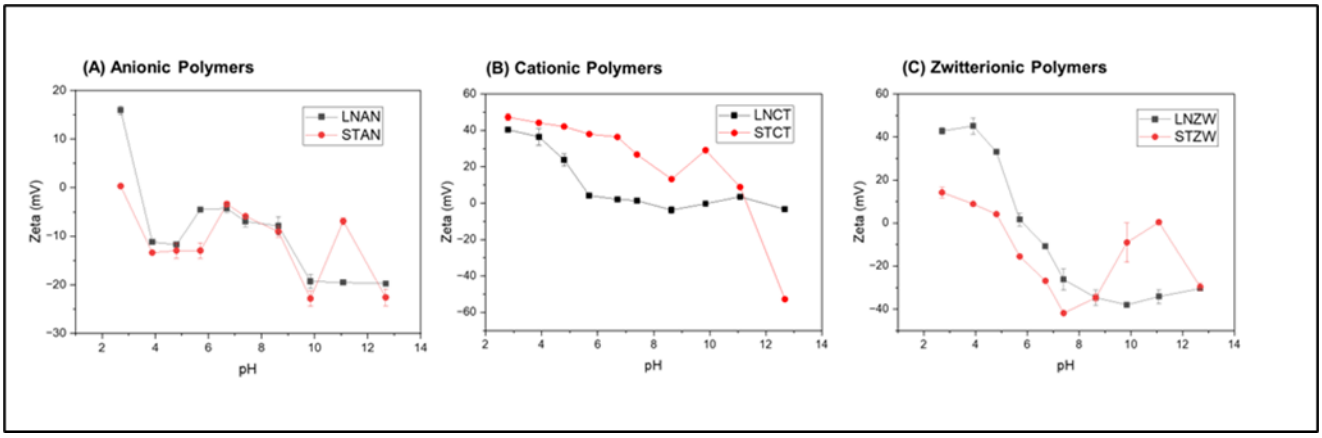

Fig 3.24 pH dependent size studies of charged polymers

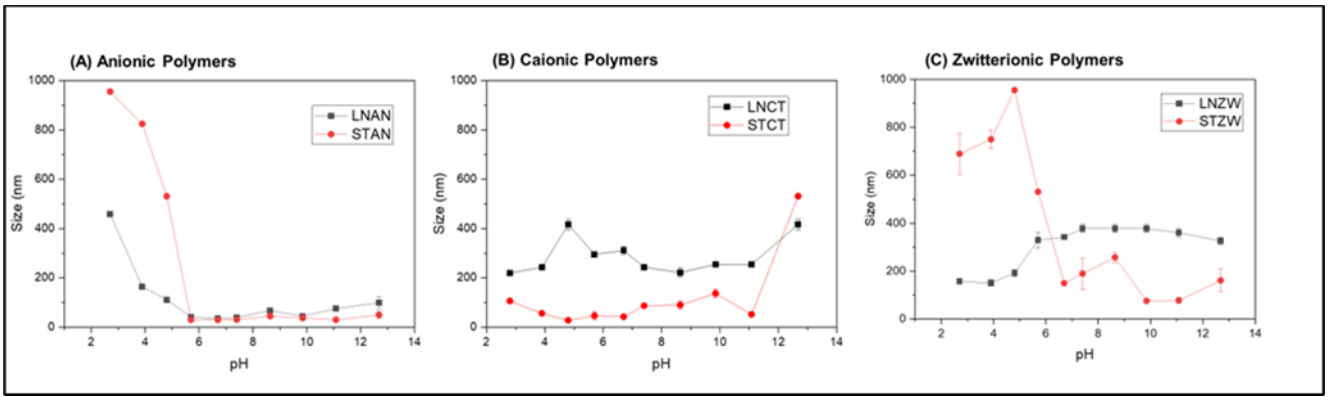

Fig 3.25 pH dependent charge studies of charged polymers

3.8 Dye encapsulation in the zwitterionic nano-scaffolds:

To study the loading efficiency of zwitterionic moieties, encapsulation of HPTS, an anionic dye was done using dialysis method to remove DMSO and unencapsulated dye. UV-visible spectroscopy was employed to ensure the difference in the drug loading capabilities of linear and star zwitterionic scaffolds. Drug loading content and drug loading efficiency were found to be more for linear polymer than the star polymer. This could be due to the role of topology and charges in the polymer backbone. The overall effect is favoring the more loading capabilities in case of linear zwitterionic polymers. Further, the size differences and shift in zeta potential after HPTS encapsulation showed more significant change, indicating their less stability. The observation of small changes in the size after encapsulation confirmed the stability of linear nanoparticles. Further, the charge variation in linear polymer from -33mV to -35 mV monitored by Zeta potential ensured the better interaction and occupancy of dye in this case.

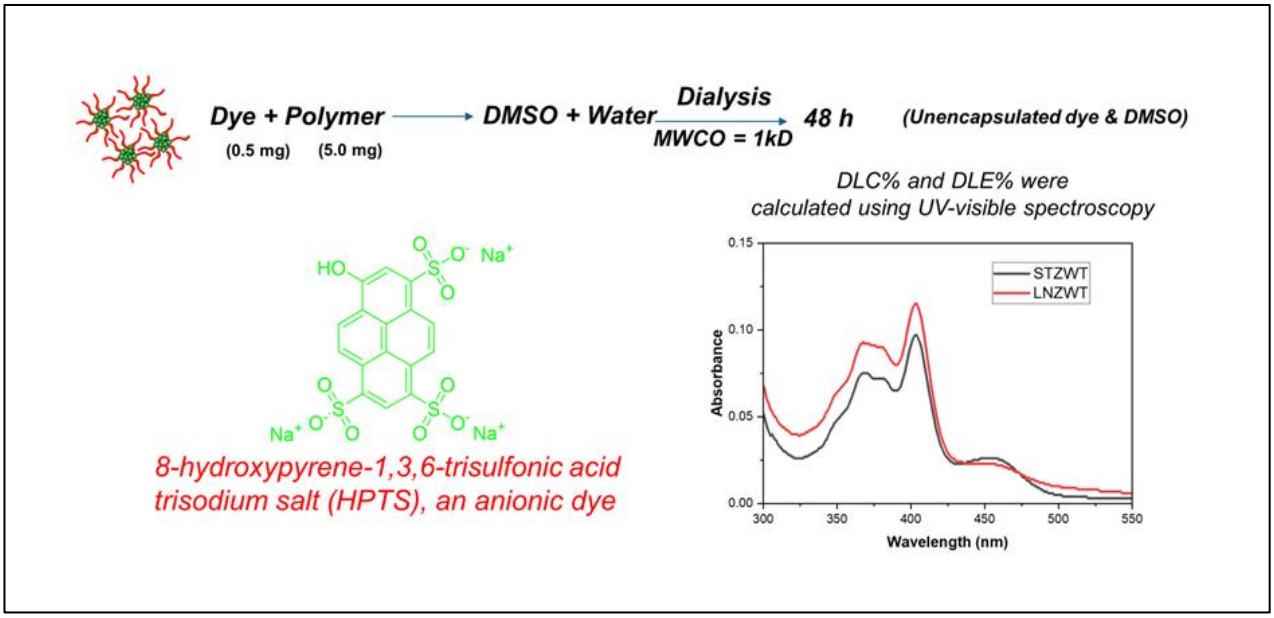

Fig 3.26 Dye Encapsulation in Zwitterionic nano-scaffolds

Polymers	Size (nm)	Zeta Potential (mV)	PDI	Size (nm) After encapsulation	Zeta Potential (mV) After encapsulation	PDI After encapsulation	DLC %	DLE %
LN-zwi	326±20	-33±0.5	0.5±0.01	342	-35±0.4	0.3±0.05	3.35	33.48
ST-zwi	175±30	-29±0.7	0.3±0.04	268±18	-18±0.3	0.3±0.02	2.82	28.25

Table 2: Changes before and after dye encapsulation

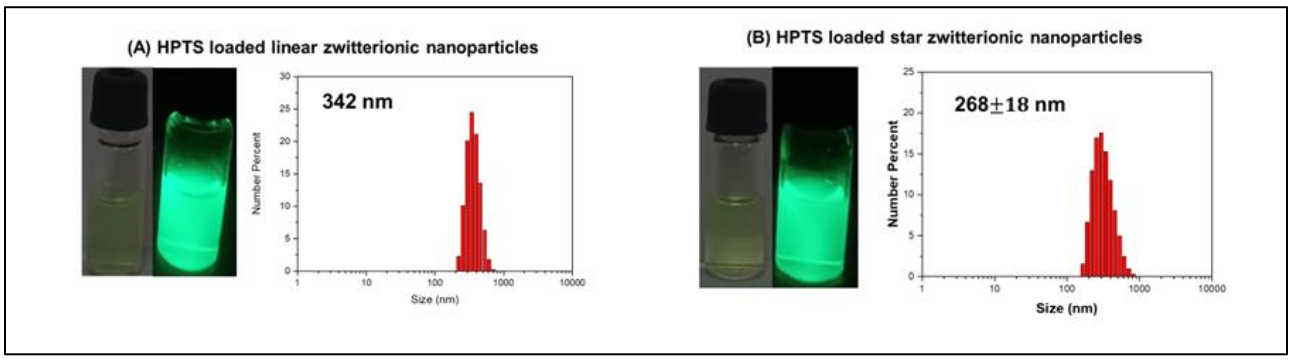

Fig 3.27 HPTS loaded zwitterionic nanoparticles

Chapter 4 Conclusion

The engineering of newly developed biodegradable based cationic, anionic and zwitterionic linear and star polymer have been done. Further, the role of topology and charges have been explored, and significant differences in the self-assemblies have been observed. The comparison of linear polymer with degree of polymerization, Xn=10, has been compared to the star polymers having Xn=60, statistically 10 units on each arm. Linear and star zwitterionic polymers were employed for drug encapsulation capabilities. The overall effect of topology, stability and charges favors the more amount of drug encapsulation in the case of linear zwitterionic polymer nanoparticles. The pH dependent studies confirmed the more stability of linear zwitterionic polymers than the star zwitterionic polymers. The newly synthesized zwitterionic polymers based on caprolactone show a potential to fabricate them for drug delivery vehicles in anticancer treatment. Further, the control on topology and charge plays a crucial role in the stability and drug loading efficiency. The smart fabrication of zwitterionic polymers based on substituted polycaprolactones have opened the access to develop structure modified biodegradable polymers for various biomedical applications.

REFERENCES:

(1) Theodorou, I. G.; Mpekris, F.; Papagiorgis, P.; Panagi, M.; Kalli, M.; Potamiti, L.; Kyriacou, K.; Itskos, G.; Stylianopoulos, T. Gold Nanobipyramids for Near-Infrared Fluorescence-Enhanced Imaging and Treatment of Triple-Negative Breast Cancer. *Cancers (Basel)* **2023**, *15* (14). https://doi.org/10.3390/cancers15143693.

(2) Soliman, G. M.; Sharma, A.; Maysinger, D.; Kakkar, A. Dendrimers and Miktoarm Polymers Based Multivalent Nanocarriers for Efficient and Targeted Drug Delivery. *Chemical Communications* **2011**, *47* (34), 9572–9587. https://doi.org/10.1039/c1cc11981h.

(3) Maeda, H.; Nakamura, H.; Fang, J. The EPR Effect for Macromolecular Drug Delivery to Solid Tumors: Improvement of Tumor Uptake, Lowering of Systemic Toxicity, and Distinct Tumor Imaging in Vivo. *Advanced Drug Delivery Reviews*. January 2013, pp 71–79. https://doi.org/10.1016/j.addr.2012.10.002.

(4) Erfani, A.; Seaberg, J.; Aichele, C. P.; Ramsey, J. D. Interactions between Biomolecules and Zwitterionic Moieties: A Review. *Biomacromolecules* **2020**, *21* (7), 2557–2573. https://doi.org/10.1021/acs.biomac.0c00497.

(5) Xu, S.; Nilles, J. M.; Bowen, K. H. Zwitterion Formation in Hydrated Amino Acid, Dipole Bound Anions: How Many Water Molecules Are Required? *Journal of Chemical Physics* **2003**, *119* (20), 10696–10701. https://doi.org/10.1063/1.1620501.

(6) He, Y.; Hower, J.; Chen, S.; Bernards, M. T.; Chang, Y.; Jiang, S. Molecular Simulation Studies of Protein Interactions with Zwitterionic Phosphorylcholine Self-Assembled Monolayers in the Presence of Water. *Langmuir* **2008**, *24* (18), 10358–10364. https://doi.org/10.1021/la8013046.

(7) Wu, J.; He, C.; He, H.; Cheng, C.; Zhu, J.; Xiao, Z.; Zhang, H.; Li, X.; Zheng, J.; Xiao, J. Importance of Zwitterionic Incorporation into Polymethacrylate-Based Hydrogels for Simultaneously Improving Optical Transparency, Oxygen Permeability, and Antifouling Properties. *J Mater Chem B* **2017**, *5* (24), 4595–4606. https://doi.org/10.1039/c7tb00757d.

(8) Rampado, R.; Crotti, S.; Caliceti, P.; Pucciarelli, S.; Agostini, M. Recent Advances in Understanding the Protein Corona of Nanoparticles and in the Formulation of “Stealthy” Nanomaterials. *Frontiers in Bioengineering and Biotechnology*. Frontiers Media S.A. April 3, 2020. https://doi.org/10.3389/fbioe.2020.00166.

(9) Zhai, S.; Ma, Y.; Chen, Y.; Li, D.; Cao, J.; Liu, Y.; Cai, M.; Xie, X.; Chen, Y.; Luo, X. Synthesis of an Amphiphilic Block Copolymer Containing Zwitterionic Sulfobetaine as a Novel PH-Sensitive Drug Carrier. *Polym Chem* **2014**, *5* (4), 1285–1297. https://doi.org/10.1039/c3py01325a.

(10) Zhou, L. Y.; Zhu, Y. H.; Wang, X. Y.; Shen, C.; Wei, X. W.; Xu, T.; He, Z. Y. Novel Zwitterionic Vectors: Multi-Functional Delivery Systems for Therapeutic Genes and Drugs. *Computational and Structural Biotechnology Journal*. Elsevier B.V. January 1, 2020, pp 1980–1999. https://doi.org/10.1016/j.csbj.2020.07.015.

(11) Zhang, P.; Jain, P.; Tsao, C.; Yuan, Z.; Li, W.; Li, B.; Wu, K.; Hung, H. C.; Lin, X.; Jiang, S. Polypeptides with High Zwitterion Density for Safe and Effective Therapeutics. *Angewandte Chemie - International Edition* **2018**, *57* (26), 7743–7747. https://doi.org/10.1002/anie.201802452.

(12) Pelegri-O'Day, E. M.; Bhattacharya, A.; Theopold, N.; Ko, J. H.; Maynard, H. D. Synthesis of Zwitterionic and Trehalose Polymers with Variable Degradation Rates and Stabilization of Insulin. *Biomacromolecules* **2020**, *21* (6), 2147–2154. https://doi.org/10.1021/acs.biomac.0c00133.

(13) Woodard, L. N.; Grunlan, M. A. Hydrolytic Degradation and Erosion of Polyester Biomaterials. *ACS Macro Letters*. American Chemical Society August 21, 2018, pp 976–982. https://doi.org/10.1021/acsmacrolett.8b00424.

(14) Zhang, Q.; Song, M.; Xu, Y.; Wang, W.; Wang, Z.; Zhang, L. Bio-Based Polyesters: Recent Progress and Future Prospects. *Progress in Polymer Science*. Elsevier Ltd September 1, 2021. https://doi.org/10.1016/j.progpolymsci.2021.101430.

(15) Lecomte, P.; Riva, R.; Jerome, C. Synthesis of Functionalized Aliphatic Polyesters by the "Click" Copper-Catalyzed Alkyne-Azide Cycloaddition. *NATO Science for Peace and Security Series A: Chemistry and Biology* **2009**, 77–91. https://doi.org/10.1007/978-90-481-3278-2_5.

(16) Cao, J.; Xiu, K. M.; Zhu, K.; Chen, Y. W.; Luo, X. L. Copolymer Nanoparticles Composed of Sulfobetaine and Poly(ε- Caprolactone) as Novel Anticancer Drug Carriers. *J Biomed Mater Res A* **2012**, *100 A* (8), 2079–2087. https://doi.org/10.1002/jbm.a.34120.

(17) Venkataraman, S.; Tan, J. P. K.; Ng, V. W. L.; Tan, E. W. P.; Hedrick, J. L.; Yang, Y. Y. Amphiphilic and Hydrophilic Block Copolymers from Aliphatic N-Substituted 8-Membered Cyclic Carbonates: A Versatile Macromolecular

Platform for Biomedical Applications. *Biomacromolecules* **2017**, *18* (1), 178–188. https://doi.org/10.1021/acs.biomac.6b01463.

(18) Laschewsky, A. Structures and Synthesis of Zwitterionic Polymers. *Polymers*. Molecular Diversity Preservation International 2014, pp 1544–1601. https://doi.org/10.3390/polym6051544.

(19) Blosch, S. E.; Scannelli, S. J.; Alaboalirat, M.; Matson, J. B. Complex Polymer Architectures Using Ring-Opening Metathesis Polymerization: Synthesis, Applications, and Practical Considerations. *Macromolecules* **2022**, *55* (11), 4200–4227. https://doi.org/10.1021/acs.macromol.2c00338.

(20) Zhang, M.; Yu, P.; Xie, J.; Li, J. Recent Advances of Zwitterionic-Based Topological Polymers for Biomedical Applications. *Journal of Materials Chemistry B*. Royal Society of Chemistry February 2, 2022, pp 2338–2356. https://doi.org/10.1039/d1tb02323c.

(21) Xie, W.; Jiang, N.; Gan, Z. Effects of Multi-Arm Structure on Crystallization and Biodegradation of Star-Shaped Poly(ε-Caprolactone). *Macromol Biosci* **2008**, *8* (8), 775–784. https://doi.org/10.1002/mabi.200800011.

(22) Ren, J.; Zhang, Z.; Feng, Y.; Li, J.; Yuan, W. Synthesis of Star-Shaped Poly(ε-Caprolactone)-b-Poly(L-Lactide) Copolymers: From Star Architectures to Crystalline Morphologies. *J Appl Polym Sci* **2010**, *118* (5), 2650–2658. https://doi.org/10.1002/app.32590.

(23) Javan Nikkhah, S.; Vandichel, M. Modeling Polyzwitterion-Based Drug Delivery Platforms: A Perspective of the Current State-of-the-Art and Beyond. *ACS Engineering Au* **2022**, *2* (4), 274–294. https://doi.org/10.1021/acsengineeringau.2c00008.

(24) Wang, J. L.; Dong, C. M. Physical Properties, Crystallization Kinetics, and Spherulitic Growth of Well-Defined Poly(E{lunate}-Caprolactone)s with Different Arms. *Polymer (Guildf)* **2006**, *47* (9), 3218–3228. https://doi.org/10.1016/j.polymer.2006.02.047.

(25) Surnar, B.; Jayakannan, M. Stimuli-Responsive Poly(Caprolactone) Vesicles for Dual Drug Delivery under the Gastrointestinal Tract. *Biomacromolecules* **2013**, *14* (12), 4377–4387. https://doi.org/10.1021/bm401323x.

(26) Malhotra, M.; Surnar, B.; Jayakannan, M. Polymer Topology Driven Enzymatic Biodegradation in Polycaprolactone Block and Random Copolymer Architectures for Drug Delivery to Cancer Cells. *Macromolecules* **2016**, *49* (21), 8098–8112. https://doi.org/10.1021/acs.macromol.6b01793.

(27) Ghosh, R.; Malhotra, M.; Madhuri Sathe, R. R.; Jayakannan, M. Biodegradable Polymer Theranostic Fluorescent Nanoprobe for Direct Visualization and Quantitative Determination of Antimicrobial Activity. *Biomacromolecules* **2020**, *21* (7), 2896–2912. https://doi.org/10.1021/acs.biomac.0c00653.

(28) Ghosh, R.; Jayakannan, M. Theranostic FRET Gate to Visualize and Quantify Bacterial Membrane Breaching. *Biomacromolecules* **2023**, *24* (2), 739–755. https://doi.org/10.1021/acs.biomac.2c01202.

(29) Malhotra, M.; Pune, I.; Pardasani, M.; Srikanth, P. Star-Polymer Unimolecular Micelles for Brain Specic Delivery of Anticancer Drug. https://doi.org/10.21203/rs.3.rs-2251762/v1.